1-1-2010

Thrust and bending moment of rigid piles subjected to moving soil

Wei-Dong Guo
Griffith University, wdguo@uow.edu.au

H Y. Qin
Griffith University

Thrust and bending moment of rigid piles subjected to moving soil

Abstract

An experimental apparatus was developed to investigate the behaviour of vertically loaded free-head piles in sand undergoing lateral soil movement(wf). A large number of tests have been conducted to date. Presented herein are 14 typical model pile tests concerning 2 diameters, 2 vertical pile loading levels, and varying sliding depths with the movement Wf driven by a triangular loading block. The results are provided regarding driving force, and induced shear force (T), bending movement (M) and deflection (y) along the piles with Wf/ normalised sliding depth. The tests enable simple expressions to be proposed, capitalised on theory for laterally loaded pile.

The new expressions well captures the evolution of M, T, and Y with soil movement observed in current model tests, and the ~5 times difference in maximum bending movement (Mmax) from two modes of loading. They further offer good estimation of Mmax for 8 in-situ pile tests and one centrifuge test pile. The study quantifies the sliding resistance offered by a pile for the given Wf profiles, pile location (related to boundary), and vertical load. It established the linear correlation between the maximum thrust (resistance T) and Mmax, regardless of magnitudes of Wf.

Keywords

thrust, piles, moving, moment, soil, rigid, bending, subjected

Disciplines

Engineering | Science and Technology Studies

Publication Details

Guo, W. & Qin, H. Y. (2010). Thrust and bending moment of rigid piles subjected to moving soil. Canadian Geotechnical Journal, 47 (2), 180-196.

Abstract:

An experimental apparatus was developed to investigate the behaviour of vertically loaded free-head piles in sand undergoing lateral soil movement (w_f). A large number of tests have been conducted to date. Presented herein are 14 typical model pile tests concerning 2 diameters, 2 vertical pile loading levels, and varying sliding depths with the movement w_f driven by a triangular loading block. The results are provided regarding driving force, and induced shear force (T), bending moment (M) and deflection (y) along the piles with w_f /normalised sliding depth. The tests enable simple expressions to be proposed, capitalised on theory for laterally loaded pile.

The new expressions well captures the evolution of M, T, and y with soil movement observed in current model tests, and the ~5 times difference in maximum bending moment (M_{max}) from two modes of loading. They further offer good estimation of M_{max} for 8 in-situ pile tests and one centrifuge test pile. The study quantifies the sliding resistance offered by a pile for the given w_f profiles, pile location (related to boundary), and vertical load. It establishes the linear correlation between the maximum thrust (resistance T) and M_{max}, regardless of magnitudes of w_f.

KEYWORDS: ground improvement; model tests, piles, slopes, soil/structure interaction, theoretical analysis

1. INTRODUCTION

Study on active piles subjected to combined lateral and vertical loads has attracted significantly research effort (Meyerhof et al. 1981; Meyerhof et al. 1983; Anagnostopoulos and Georgiadis 1993; Aubeny et al. 2003; Karthigeyan et al. 2007). However, limited study on response of (passive) piles owing to lateral soil movement and vertical loading is available (Knappett and Madabhushi 2009). It is not clear how the bending moment is related to maximum sliding force (lateral thrust) developed in a passive pile, in particular, once coupled with vertical loads and various soil movement profiles. The correlation needs to be established to facilitate design and inspection of piles used to stabilise slope, and to support bridge abutments and foundations of tall buildings. The study to date has principally been based on centrifuge tests (Stewart et al. 1994; Bransby and Springman 1997; Leung et al. 2000), laboratory model tests (Poulos et al. 1995; Pan et al. 2002; Guo and Ghee 2004), theoretical and numerical analyses (Ito and Matsui 1975; Viggiani 1981; Poulos 1995; Guo 2003). The results are useful in one way or another. Nevertheless, it is unfortunate that the correlation between the moment and the lateral thrust (i.e. shear force in a pile) in majority of model pile tests was not provided. The force is indeed required to evaluate maximum bending moment (Poulos 1995) in design piles in aforementioned situation.

Limit equilibrium solutions have been derived for piles in a two-layered cohesive soil (Viggiani 1981; Chmoulian and Rendel 2004). They allow maximum bending moment to be correlated to lateral thrust by stipulating (i) A fixed sliding depth; and (ii) A uniform soil movement profile (without axial load on pile-head). The solutions are popularly used for passive piles. Likewise, p-y curve based methods are widely adopted in practice. However, recent study shows that the p-y method significantly overestimated pile deflection and bending moment, and therefore further research is warranted (Frank and Pouget 2008). Response of in-situ slope stabilising piles was recorded (Esu and D'Elia 1974; Fukuoka 1977; Carrubba et al. 1989; Kalteziotis et al. 1993;

Smethurst and Powrie 2007; Frank and Pouget 2008). Among others, elastic solutions (Fukuoka 1977; Cai and Ugai 2003) and elastic-plastic solutions (Guo 2009) were developed. The former compares well with measured pile response at the reported stress states. The elastic-plastic solutions can capture well nonlinear response of passive piles at any soil movement. Nevertheless, the effect of soil movement profiles on the response is yet to be clarified, coupled with an axial load and in pre-failure state. This can be examined through model pile tests. Above all, a simple correlation between lateral thrust and maximum bending moment is needed to facilitate practical design.

Small scale experiment can bring about valuable insight into pile-soil interaction mechanism. It can clarify and quantify key parameters (Abdoun et al. 2003). To examine the response of passive piles, Guo and Ghee (2004) developed a new experimental apparatus. Extensive tests have been conducted to date on piles in sand. Some results were published previously (Guo and Ghee 2005; Guo et al. 2006). This paper presents 14 typical test results under an inverse triangular loading block, which were deduced from test piles of 2 diameters, and subjected to 2 axial load levels. They are analysed in order to:

- Establish the relationship between maximum bending moment and lateral sliding thrust.
- Simulate the evolution of the moment and the sliding thrust with moving soil.

The test results are presented in form of the profiles of bending moment, shear force and deflection along the pile against frame movement or normalised sliding depth. The measured correlation between maximum bending moment and lateral thrust, and that between the thrust and soil movement are provided. They allow newly developed expressions to be validated with respect to impact of subgrade modulus, vertical load, 2 different (translational or rotational) loading manner, and effective soil movement. The established correlations are further compared with measured data of 8 in-situ test piles and one centrifuge test pile.

2. APPARATUS AND TEST PROCEDURES

2.1. Shear box and loading system

Figure 1 shows an overview of the experimental apparatus developed in the current study. It is mainly made up of a shear box, a loading system, and a data acquisition system. The shear box measures 1 m both in length and width. The upper section of the shear box consists of 25 mm deep square laminar steel frames. The frames, which are allowed to slide, contain the "moving layer of soil" of thickness L_m. The lower section of the shear box comprises a 400 mm height fixed timber box and the desired number of laminar steel frames that are fixed, so that a "stable layer of soil" of thickness L_s (≥ 400 mm) can be guaranteed. Changing the number of movable frames in the upper section, the thicknesses of the stable and moving layers are varied accordingly. Note that the L_m and L_s are defined at loading location, and they do vary across the shear box. The actual sliding depth L_m around a test pile is unknown, but it would not affect the conclusions to be drawn in this paper.

The loading system encompasses a loading block that is placed on the upper movable laminar frames, and some weights on top of the test pile. The loading block is made to different shapes in order to generate various soil movement profiles. The triangular loading block employed herein has an (loading) angle of 16.7^o (see Fig. 2). A translational frame movement of w_f will induce an increasing sliding depth of $3.33w_f$ (at the loading location) until a pre-specified final depth of L_m. Thereafter, additional frame movement will be uniform over the depth L_m, resulting in an overall trapezoid soil movement profile. A hydraulic jack is used to drive the loading block. The jack stroke permits a lateral frame movement w_f up to 150 mm. Response of the pile is monitored via strain gauges distributed along the piles (see Fig. 2a), and via two linear variable displacement transducers (LVDT) above the model ground (Fig. 1). The test readings are recorded and processed via a data acquisition system and a computer, which are transferred into 'measured' pile response using a purposely-designed program discussed later on.

2.2. Sample preparation and sand properties

Medium oven-dried quartz sand was utilised in this study. Fig. 3 shows its particle size distribution, which has an effective grain size D_{10} = 0.12 mm, a uniformity coefficient C_u = 2.92, and a coefficient of curvature C_c = 1.15. The sand was rained into the shear box through a rainer hanging over the box. The falling height is selected to generate a uniform and desired density, which in this study was chosen as 600 mm. This is supposed to offer a relative density of 89% and a unit weight of 16.27 kN/m^3 (see Fig. 4). Angle of internal friction of the sand is 38˚ as evaluated from direct shear tests.

2.3. Model pile

The aluminium pipe piles tested had a length of 1,200 mm, see Fig. 2(a). They were made of two configurations: One has an outer diameter (d) of 32 mm, a wall thickness (t) of 1.5 mm, and a flexural stiffness (E_pI_p) of 1.17 kNm^2; while the other has d = 50 mm, t = 2 mm, and E_pI_p = 6.09 kNm^2. Ten levels of strain gauges were placed on the pile surface at an interval of 100 mm. They were calibrated prior to the tests. This is done by applying a transverse load in the middle of the pile clamped at both ends. Each gauge reading measured under various loads is then compared with theoretically calculated strain. A calibration factor is thus obtained for each gauge, which permits the gauge readings to be converted to actual strains. During the pile test, the strain gauges were protected from damage by covering with 1 mm of epoxy and being wrapped with tapes.

2.4. Test programme

A series of tests were conducted to date using the triangular loading block. 14 typical tests are presented herein as summarized in Table 1. Each test is denoted by two letters and two numbers, e.g. TS32-0 and TD32-294: (i) The triangular loading block is signified as *T*; (ii) The ‘S’ and ‘D’ refer to a pre-selected sliding depth (L_m) of 200 mm and 350 mm, respectively; (iii) The ‘32’

indicates 32 mm in diameter, and (iv) the '0' or '294' represents without or with an axial load of 294 N, respectively. Three types of 'Pile location', 'Standard' and 'Varying sliding depth' tests are reported herein:

- 'Pile location' tests were carried out to investigate the impact of relative distance between the loading block and pile location etc; 'Standard' tests were performed to explain response to the two final pre-selected sliding depths of 200 mm and 350 mm; and 'Varying sliding depth' tests were done to highlight bending moment raises owing to additional movement beyond the triangular profile.

For each test, firstly, the sample model ground was prepared in a way described previously to a depth of 800 mm. Secondly, the instrumented pile was jacked in continuously to a depth of 700 mm below the surface, while the (driving) resistance was monitored. Thirdly, an axial load was applied on the pile-head using a number of weights (to simulate a free-head pile condition) that were secured (by using a sling) at 500 mm above the soil surface. Fourth, the lateral force was applied via the triangular block on the movable frames to enforce translational soil movement towards the pile. And finally, the sand was emptied from the shear box after each test.

During the passive loading, the gauge readings, LVDT readings and the lateral force on the frames were generally taken at every 10 mm movement of the top laminar steel frame (e.g. frame movement, w_f) to ~150 mm. A number of trial tests prove the repeatability and consistency of test results presented herein.

2.5. Determining pile response

A spreadsheet program via Microsoft Excel VBA was written to process and analyze the data obtained from strain gauges and LVDTs. The inclination and deflection profiles along the pile were derived, respectively from 1st and 2nd order numerical integration of the bending moment profile. The shear force, and soil reaction profiles were deduced by using single and double numerical differentiation of the bending moment profile, respectively. With this program, typical

response profiles of bending moment, shear force, soil reaction, deflection and rotation profiles (Guo and Qin 2006) were deduced for all the tests. They allow the following response to be gained for typical frame movement w_f : maximum bending moment M_{max}, depth of the moment d_{max}, maximum thrust (shear force in the pile) $T_{\max}$, and pile deflection at groundline y_t (see Table 1).

2.6. Influence factors on test results

The current test apparatus allows non-uniform mobilisation of soil movement across the shear box. The resulting impact is revealed by the 'pile location' tests. A pile (with d = 32 mm) was installed at a distance s_b of 340 mm, or 500 mm, or 660 mm from the loading jack side. For instance, the s_b of 500 mm is for a pile installed at the centre of the box. Driving the loading block at the pre-specified final sliding depth of 200 mm, three tests were conducted. The $M_{\max}$ obtained is plotted against s_b in Fig. 5. It shows a reduction of ~ 32 kNmm (at w_f = 70~80 mm) in the moment as the pile was relocated from s_b = 340 mm to 500 mm, and a reduction of ~ 10 kNmm from s_b = 500 mm to 660 mm. The total maximum moment was 45~50 kNmm for the pile tested at the centre of the box. All the piles reported subsequently were tested at the centre.

3. TEST RESULTS

3.1. Driving force and lateral force on frames

The jack-in forces for six typical tests were recorded during the installation. They were plotted in Fig. 6. The figure shows more or less linear increase in driving force with the pile penetration. At the final penetration of 700 mm, the average total forces of the same diameter piles reach 5.4 kN (d = 50 mm piles) and 3.8 kN (d = 32 mm piles), respectively, with a variation of ~ ±20%. This reflects the possible variations in model ground properties, as the jack-in procedure was consistent. (Note the axial load of 294N on the pile head was 7~9% the final jacking resistance).

The average shaft friction for the installation is estimated as 54 kPa (d = 32 mm) and 49.1 kPa (d = 50mm), respectively, ignoring the end-resistances on the open-ended piles.

Total lateral force on the frames was recorded via the lateral jack during the tests upon each 10 mm frame movement (w_f). They are plotted in Fig. 7 for the six tests. Figs. 8a-8g provide the photos taken during the test TS50-294 for a few typical w_f. Fig. 7 demonstrates the following:

- The force in general linearly increases with the frame movement until it attains a constant.
- Shear modulus of the sand G_s is deduced as 15~20 kPa using the linear portion of each force-movement curve. For instance, with the TS test series, the maximum shear stress τ is estimated as 4.5~5.0 kPa (= 4.5~5.0 kN on loading block /shear area of 1.0m^2). The maximum shear strain γ is evaluated as 0.25~0.3 (= w_f/L_m, with w_f = 50~60 mm and L_m = 200 mm), assuming the shear force is transferred across the sliding depth L_m of 200 mm. The ultimate shear resistance offered by the pile is ~ 0.6 kN (see Fig. 9), which accounts for ~10% the total applied force of 5~8 kN on the frames. The determined shear stress and modulus thus may be reduced by ~10% for the tests without the pile.
- The average overburden stress σ_v at the sliding depth of 200 mm is about 1.63 kPa (= 16.3×0.1). At this low stress level, sand dialatancy is evident, which generates a number of 'heaves' (see Fig. 8h).
- Lateral force attained maximum either around w_f = 50~60 mm (TS series) or around 90~120 mm (TD series), and dropped slightly afterwards. The slight fluctuation in the force at large frame movements reflects stress build-up and redistribution around the pile featured by the gradual formation of 'heaves'. The pile response, however, attained maximum at a higher w_f of either 70~90 mm (TS series) or 120 mm (TD series) shown later on, indicating a difference of ~30 mm in w_f (i.e. w_i shown later) in transferring the applied force to the pile.

Figure 8 shows the sequential frame movements in lateral and vertical dimensions as the loading block advances. Table 2 shows the typical $\boldsymbol{w_f}$ and the sliding depth induced. A sliding depth ratio

R_L is defined herein as the ratio of thickness of moving soil (L_m) over the pile embedment length (i.e. $L = L_m + L_s$). It is utilized later to quantify the impact of depth of moving layer. For instance, in the TS test series, a $w_f \leq 60$ mm would correspond to a triangular profile to a sliding depth L_m of 200 mm, otherwise to a trapezoid soil movement profile with a constant $R_L = 0.29$.

3.2. Response of M_{max}, d_{max}, y_t versus w_i (w_f)

Figure 10 shows the profiles of bending moment, shear force and pile deflection deduced from the test on the 32 mm diameter pile without axial load (TS32-0). Fig. 11 provides the same profiles for the test on the pile with a load of 294 N (TS32-294). They reflect the impact of the triangular movement profile for $w_f \leq 60$ mm and that of trapezoid profile afterwards. Critical responses of maximum bending moment M_{max}, the depth d_{max}, and the head deflection at groundline y_t are obtained and highlighted below:

- At the maximum response state and without axial load (TS32-0): $M_{max} = 49.7$ kNm, $d_{max} = 370$ mm, and $y_t = 10$ mm. The pile mainly rotated (see Fig. 10) about the pile tip.
- Imposing the axial load, the M_{max} increases to 78.6 kNmm (i.e. 60% increase compared to without load) (see Fig. 11). Negative bending moment was observed around sand surface at the initial stage with $w_f = \sim 40$ mm ($R_L < 0.17$). The pile rotated about a depth of 550 ~ 700 mm (pile-tip level), and induced a deflection y_t of ~13 mm (i.e. 30% increase).

Strongest response profiles are observed at $w_f = 70$ ~90 mm (d =32 mm) for the two tested piles. They are plotted in Figs. 12a and 12b along with those reported previously for $d = 50$ mm (Guo and Qin 2006). The evolution of the maximum bending moment M_{max} and shear force T_{max} are furnished in Figs. 13a and 13b against the movement w_f (for d = 50 mm and 32 mm), respectively. The figures demonstrate the following.

- A small thickness of moving soil (with $R_L < 0.17$, thus $L_m < 120$ mm) did not render sand to move around the piles located at $s_b = 500$ mm. The initial frame movement w_f (denoted by

w_i hereafter) of 37 mm causes trivial response on each of the four test piles. An effective frame movement should be w_f - w_i (mm).

- As the w_f increases from 37 to 80 mm (R_L = 0.17~0.29), the M_{max} for all tests increases proportionally, irrespective of the axial loads, perhaps the w_f is prevailed by a triangular soil movement profile. At higher w_f (> 80~90 mm), the M_{max} maintains at a constant and conforms to a trapezoid soil movement.
- Given w_f = 37~80 mm, the M_{max} in tests with the axial load (e.g. TS32-294, and TS50-294) exhibits a 'delayed' stiff increase and attains a high ultimate value, compared to the pile without the load. (The effect is more remarkable for deep sliding case, as shown subsequently). A 60% increase in the M_{max} owing to the axial load for the 32 mm diameter pile is noted compared to 30% for the 50 mm diameter piles.

The w_i captures the impact of the evolution of strain wedges carried by the loading block. For instance, at w_f = 30 mm, L_m =105 mm, the lateral extent (at surface) of the wedge is calculated as 225 mm [= 105 tan(45^o+40^o/2), the frictional angle of 40^o is used to cater for the compaction effect associated with the moving]. This extent is vindicated by the few 'heaves' mentioned earlier (see Fig. 8h). The correlation between maximum shear force T_{max} and the M_{max} is discussed later on.

3.3. Response at 'Deepest' sliding depth

Figures 14 and 15 provide the response profiles obtained using the deepest pre-selected sliding depth of 350 mm and the triangular loading block (TD32-0 and TD32-294). Without the axial load, the 32 mm diameter pile principally rotated about the middle pile embedment, and the y_t reached 46 mm at w_f = 110 mm. Imposing the axial load of 294 N (TD32-294), the same size pile translated and rotated around the pile tip and the y_t reached 62.5mm. The moment and shear force profiles for the 32 mm piles and the 50 mm piles at maximum state (w_f = 120 mm) are depicted in Figs. 16a and 16b, respectively. The evolution of the maximum bending moments

and shear forces with the advance of the frames is illustrated in Figs. 17a and 17b. These figures show the following features:

- Reaction from the 50 mm piles is negligible within a w_i of 30 mm, which is less than 37 mm for d = 32 mm piles
- The axial load causes constant bending moments down to a depth of 200 mm (Fig. 16), below which, the moment distribution resembles that from TS tests (Fig. 12); and it renders the M_{max} increase to ~143 kNmm (see Fig. 16) that occurs at a depth d_{max} of 0.465m.
- The thrust T_{max} and the M_{max} in the pile will in general attain higher values than these seen in the figures, as the movement w_f of 120 mm just mobilises a sliding depth L_m of 350 mm (see Table 2).

3.4. Progressive moving sand on M_{max}

The evolution of M_{max} with the normalised sliding depth R_L is given in Fig. 18a. It shows three distinct stages: A small value of M_{max} at $0 \le w_f < 37$ mm ($R_L < 0.17$); the linear increase in M_{max} owing to the triangular movement profile with 37 mm $\le w_f <$ 60 mm (L_m = 200 mm, R_L = 0.29) or with 37 mm $\le w_f <$ 120 mm (L_m = 350 mm, R_L = 0.5); and the moment raises at either R_L = 0.29 or 0.5 that caused by uniform movement beyond the triangular movement. The moment raises were determined by conducting 4 more tests on the piles (d = 32 mm) to the pre-selected final sliding depths of 125(R_L = 0.179), 250(0.357), 300(0.429) and 350 mm (0.5), (without axial load), respectively. The magnitudes of M_{max} obtained are 5.2, 62.6, 115.3, 118.1 kNmm upon initiating the trapezoid profile (see Table 2). They finally reached 5.7, 123.5, 175.0, and 140.0 (not yet to limit) kNmm, respectively. These values are plotted in Fig. 18b against the R_L, together with the TS32-0 test. The M_{max} along with d_{max}, T_{max} and y_t are also provided in Table 1. Note that the M_{max} and T_{max} from T32-0 (L_m = 350 mm) at w_f = 120 mm are 1.2% and ~5% less than those from TD32-0, showing the repeatability and accuracy of the current tests.

4. SIMPLE SOLUTIONS

4.1 Relationship between M_{max} and T_{max}

Guo (2008b,2009) demonstrated that analytical solutions for laterally loaded (active) piles can be employed to study passive piles subjected to soil movement, for which, the lateral load P is taken as the maximum sliding force, T_{max} induced in a pile. This use with particular reference to rigid piles is further corroborated using the measured correlation between the M_{max} and the T_{max}, and that between the effective y_o (= $w_f - w_i$) and the T_{max}.

Solutions for active rigid piles

Given a free-head, floating-base, laterally loaded pile, elastic solutions offer (Scott 1981)

[1] $$M_{max} = (0.148\sim0.26)PL \quad \text{and} \quad d_{max} = (0.33\sim0.42)L$$

where P is lateral load applied at pile-head level; and d_{max} is depth of maximum bending moment. The coefficient of 0.33 or 0.148 is used for a uniform k, while 0.42 or 0.26 is for a Gibson k. For the pile, elastic-plastic solutions provide the following correlation (Guo 2008a)

[2] $$M_{max} = (\frac{2}{3} d_{max} + e)P$$

where e is the real or fictitious free-length of the lateral load above the ground surface. Eq. [2] is of identical form to that developed for laterally loaded piles at ultimate state (Broms 1964).

Use of equivalent load for passive piles

Equations [1] and [2] are used for passive piles by replacing load P with T_{max}. This is justified from two new experimental outcomes, in addition to the similarity of on-pile force profiles between passive and active loading revealed previously (Guo 2003; Guo 2008b).

- Bending moment profile for the passive piles (see Figs. 12a and 16a) shows that d_{max} = 0.35~0.4 m or (0.5~0.6)L, such that $M_{max} = (0.33\sim0.4)LT_{max}$.

- The correlation between T_{max} and M_{max} is observed as linear for all the current model tests, as is demonstrated in Figs. 19a and 19b and for almost all the w_f. Using $P = T_{max}$ in eq. [2] to fit the measured data in Figs. 19a and 19b allows $M_{max} = 0.357\ T_{max}L$ to be gained.

Points 1 and 2 indicate an elastic-plastic pile-soil interaction for the current model piles, and eq. [1] can be rewritten as

[3] $$M_{max} = (0.148\sim0.4)T_{max}L$$

4.2 Equivalent elastic solutions for passive piles

The current model tests on passive piles support the following hypotheses:

- The distance between the pile and the loading block s_b renders a remarkable portion of initial frame movement w_i of 30~37 mm to cause rather small reaction in the pile.
- The effective frame movement of w_f–w_i (= y_o) causes the groundline deflection y_t during the passive loading process. Any pile-soil relative rigid movement is incorporated into the w_i and modulus of subgrade reaction k. The y_o may be grossly estimated by using elastic theory for a lateral pile in a homogenous soil featured by

[4] $$y_o = 4T_{max}/(kL)$$

where $k = (2.4\sim3)G_s$ (Guo 2008a). The 'k' here is proportional to pile diameter d, as is noted in later calculation.

These observations offer:

[5] $$T_{max} = (w_f - w_i)kL/4$$

And Eq. [3] may be recast into

[6] $$M_{max} = (w_f - w_i)kL^2/(10\sim27)$$

where w_i is the initial frame movement which depends on the s_b, pile diameter, and loading manner. For instance, w_i = 0.03~0.037 m (the current translational tests), and w_i = 0.0 for the rotational tests reported by Poulos et al (1995). The value of 15.38~27 corresponds to elastic case of Gibson ~ constant k, whereas a value of 11.2 or 10 is adopted for that shown in Fig. 19

and the rotating tests, respectively. Later on, all 'elastic calculation' is based on a value of 15.38 (Gibson k) unless specified. The length L for each pile was taken as the smallest values of L_i (pile embedment in i^{th} layer, i = 1, 2 for sliding and stable layer respectively in this paper) and L_{ci}. For model tests, as sliding layer is not evident around a test pile, the length L has to be taken as the pile embedment length. The L_{ci} is given by (Guo and Lee 2001)

[7] $$L_{ci} = 1.05d(E_p / \overline{G}_s)^{0.25}$$

where E_p = Young's modulus of an equivalent solid cylinder pile; $\overline{G}_s$ = average shear modulus of soil over the depth of i^{th} layer. In using the expressions, it must stress that

- The modulus k is deduced from overall sliding process characterised by the sand–pile-shear box interaction. This should not be adopted for predicting pile deflection at groundline y_t and for those provided in Table 1 that reflect a local pile-soil interaction (Guo 2008b). A higher modulus k is generally seen for predicting y_t than the k for overall sliding, especially for a local pile-soil interaction (shallow sliding depth). Pile deflection y_t in the overall sliding process does encompass a significant component of 'rigid' rotation, while it does not in the local interaction. Two local-interaction cases are as follows: (i) the deflection at groundline y_t was measured as 46 mm for TD32-0 under w_f = 110 mm. Given the measured T_{max} = 0.4 kN, k = 50 kPa, and L = 0.7 m, eq. [4] yielded a similar deflection y_o of 45.7 mm. (ii) The y_o at w_f = 110 mm was evaluated as 63.5 mm for TD32-294, in light of the measured T_{max} = 0.5 kN, k = 45 kPa, and L = 0.7 m, which also compares well with the measured y_t of 62.5 mm. As expected, the values of k used here are higher than those adopted for overall-interaction illustrated in Fig. 17b.
- The estimated T_{max} and M_{max} must be capped by those deduced for ultimate state (Guo 2008b).

4.3. Example calculations of M_{max}

The current tests were conducted by translational movement of the loading block that has a loading angle of 16.7°. The sliding depth increases with the movement. The previous model pile tests (Poulos et al. 1995) were carried out by rotating loading block (rotational loading) about a constant sliding depth for each test. The current tests were generally associated with an effective soil movement y_o of 30~70 mm (= w_f -37 (mm) in Table 3), similar to the movement of 37 mm (R_L < 0.5) or 60 mm (R_L> 0.5) enforced previously (Poulos et al. 1995). Nevertheless, Fig. 18 shows a 3~5 times difference in the magnitudes of the measured bending moment M_{max} between the current and the previous tests. This difference/impact is investigated herein from 3 aspects using eqs. [5] and [6].

(1) TS, TD tests and *k*: The measured curves of M_{max} ~ w_f and T_{max}~ w_f (see Figs. 13 and 17) were simulated regarding the pre-specified final sliding depths of 200 mm (TS tests) and 350 mm (TD tests), respectively. Elastic theory offers (Guo 2008a): k/G_s = 2.841 (d = 50 mm) and 2.516 (d = 32 mm). The G_s was deduced previously as 15~21 kPa, thus the k was obtained as 45~60 kPa (d = 50 mm). Given w_i = 30 mm (TD50-294) and 37 mm (TS50-294), the moment is thus calculated using $M_{max} = (w_f - w_i)kL^2/11.2$. They agree well with the measured data shown in the figures. As the diameter is changed to 32 mm, the k reduces to 25~35 kPa, in view of its proportional reduction to the diameter (resulting in 28.8~ 38.4 kPa), and further to the ratio of 2.516/2.841. This k offers good estimations for the d = 32 mm tests as well, as shown in the figures. Eqs. (4) –(6) are thus sufficiently accurate for the deep and shallow sliding cases.

(2) Translational loading with variable sliding depths (constant L): The measured M_{max} of the piles TD32-0 and T32-0 (L_m = 350, Table 1) tested to a final sliding depth of 350 mm is presented in Table 3. It is modelled using $M_{max} = (w_f - 0.037)kL^2/11.2$, and k = 35 kPa. The estimated M_{max} for a series of w_f (or R_L) are also provided in Table 3 and plotted in Fig. 18a. The R_L was based on actual observation during the tests, which may be slightly different from the

calculated one using $R_L = 0.33w_f/L$. The same calculation is also plotted in Fig. 18b. Especially the moment raise at $R_L = 0.5$ (for w_f >120 mm) was estimated using an additional movement of 30 mm beyond the w_f of 120 mm to show the (capped) ultimate value (Guo 2008b). Table 3 shows the calculated agrees with the two sets of measured M_{max}, in view of using the same w_i of 37 mm for either test.

(3) Rotational loading about a fixed sliding depth: The M_{max} was obtained in model pile tests by loading with rotation about a fixed sliding depth (thus a typical R_L) (Poulos et al. 1995). The results for a series of R_L were depicted in Fig. 18b, and are tabulated in Table 4. This measured M_{max} is simulated via the following steps:

- The ratio of k/G_s was obtained as 2.39~2.79 using the closed-form expression by Guo and Lee (2001), which itself is a function of a factor γ (= $1.05d/L$).
- Shear modulus was stipulated as G_s =10z (G_s in kPa, z = L_s+L_m in m), from which the k was thus calculated.
- With $w_i = 0$ (as observed), the T_{max} was estimated using eq. [5] for w_f = 37 mm ($R_L < 0.5$) or w_f = 60 mm ($R_L > 0.5$), respectively
- The M_{max} was calculated as $M_{max} = w_f kL^2/10$ as per eq. [6].

The test piles are of lengths 375~675 mm, and the G_s was 3.75~6.75 kPa. The values of the M_{max} calculated for the 10 model piles are provided in Table 4. They are plotted against the ratio R_L in Fig. 18b, which serve well as an upper bound of all the measured data.

Overall, eqs. (5) and (6) offer good estimations of M_{max} (thus T_{max}) for all the current 12 model piles (e.g. Table 3) and the previous 10 tests (e.g. Table 4). The 3~5 times difference in the M_{max} is likely owing to the dominant impact of the pile dimensions (via the L and the ratio k/G_s), the subgrade modulus k, the effective movement (w_f-w_i), and the loading manner (w_i).

4.4. Calibration against in-situ test piles

The simple correlations proposed herein are validated using measured response of 8 in-situ test piles and one centrifuge test pile subjected to soil movement. The pile and soil properties are tabulated in Table 5, along with the measured values of the maximum bending moment M_{max}. The shear force T_{max}, however, was measured for 3 of the 9 piles. The T_{max} for the rest 6 piles was thus taken as that deduced using elastic and elastic-plastic theory (Cai and Ugai 2003; Guo 2009). Modulus of subgrade reaction k_i, and equivalent length of rigid pile L_{ci} were calculated previously (Guo 2009). The length L for each pile was taken as the smallest values of L_i and L_{ci}. This allows the ratio $M_{max}/(T_{max}L)$ for each case to be evaluated. The results are tabulated in Table 5, and are plotted in Fig. 20. The ratios all fall into the range of the elastic solutions capitalised on constant k to the plastic solution of eq. [3]. The slightly higher ratio for the exceptional Katamachi-B is anticipated (Guo 2009). It may argue that 4 piles with a ratio of 0.26-0.4 exhibit elastic-plastic pile-soil interaction and with an eccentricity greater than 0.

Figure 19 shows the ratio $M_{max}/(T_{max}L)$ from model pile tests stays almost invariably at 0.357 from initial to ultimate loading state. The same ratio for the in-situ pile (Frank and Pouget 2008) was calculated, for sliding and stable layer, respectively, with respect to the 'Pre-pull back' (behaving as free-head) and 'After-pull back (fixed-head)' situation for the 16 years' test duration. It is plotted in Fig. 21. The ratio for the pile in sliding layer stays around 0.25. (Note the ratio for stable layers as plotted in Fig. 21 seems to be complicated, but it is beyond the scope of this paper). In brief, the ratio $M_{max}/(T_{max}L)$ is independent of loading level for either the model tests or the field test.

Determination of the T_{max} is however, more pertinent to pile-head or base constraints. A fully fixed head observes $y_t = T_{max}/(kL)$ (Guo and Lee 2001), and a semi-fixed head follows $y_t = (1\sim4)T_{max}/(kL)$.

- The in-situ pile (Frank and Pouget 2008) at pre-pull back situation is evaluated using the free-head solution. The k was obtained as 8.8 MPa (= $100s_u$, undrained shear strength s_u = 88 kPa). At a groundline deflection y_t = 32 mm (recorded on 05/07/1995), the T_{max} was estimated as 478.7 kN (= $y_t kL/4$). This T_{max} agrees well with the measured load of 487 kN. Note the measured pile deflection increases approximately linearly from groundline to a depth of 6.8~8.0m, exhibiting 'rigid' characteristics.
- Calculation of deflection and bending moment for rigid piles is illustrated in light of the two-row piles used to stabilise a sliding slope (Kalteziotis et al. 1993). The steel piles had a length of 12 m, an external diameter of 1.03 m, a wall thickness t of 18 mm, and a flexural stiffness E_pI_p of 1,540 MNm^2. Given $k = k_1$ =15 MPa (Chen and Poulos 1997), and an equivalent rigid pile length $L = L_1$ = 4 m (sliding depth), it follows T_{max} = 45 kN (= $y_t kL/4$) at y_t = 0.003 m. This T_{max} compares well with the measured 40~45 kN. The T_{max} gives a uniform on-pile force per unit length of 10-11.25 kN/m. The moment is thus estimated as 80~90 kNm(= 0.5*(10~11.25)*4^2) about the sliding depth, and as 180~202.5 kNm about the depth 6 m. The average moment agrees well with the measured 150 kNm, considering that the depth of sliding may be 4-6 m (Chow 1996; Chen and Poulos 1997).

5. CONCLUSIONS

An experimental apparatus was developed to investigate the behaviour of vertically loaded free-head piles in sand undergoing lateral soil movement. A large number of tests have been conducted to date. Presented herein are 14 typical tests concerning 2 diameters (32 and 50 mm), 2 loading levels (0 and 294 N, 7-9% the driving force), and varying sliding depths enforced by a triangular loading block. The results are provided regarding the applied force, the induced shear force, bending moment and deflection along the piles. The tests enable simple solutions to be proposed for predicting the pile response.

The model tests show the following features:

- The M_{max} is largely linearly related to the sliding force T_{max}, even for the initial frame movement up to w_i and the extra large w_f for trapezoid movement profile.
- Maximum bending moment increases by 60% for the 32 mm diameter piles or 30% for the 50 mm piles, and its depth by ~50%, upon applying a static load of 7-9% the maximum driving force.
- 3~5 times different bending moment can occur given similar size of model piles but different loading manner.

With respect to the solutions, the following can be drawn.

- Equation [6] may be used to estimate the maximum bending moment M_{max}, for which the sliding thrust T_{max} is calculated using eq. [5]. The estimation should adopt an effective frame movement of w_f-w_i, in which the w_i depends on the pile diameter, pile position, and loading manner.
- The subgrade modulus k may be estimated using the theoretical ratio of k/G_s and the shear modulus G_s (e.g. 15~20 kPa in the current tests). The G_s is pertinent to either overall shear process of the pile-soil-shear box system or local pile-soil interaction. The k varies with diameter and should be considered accordingly.
- Capitalized on equivalent elastic pile-soil interaction, the T_{max} from eq. [5] must be capped by ultimate plastic state.

The current simple solutions, although approximate, offer satisfactory estimations of the 3~5 times different M_{max} recorded in the current and previous model pile tests; and the correct ranges of $M_{max}/(T_{max}L)$ for 8 in-situ test piles and a centrifuge test pile.

6. ACKNOWLEDGEMENTS

The work reported herein was supported by an Australian Research Council Discovery Grant (DP0209027). The financial assistance is gratefully acknowledged. The authors would like to thank Mr. Enghow Ghee for his assistance to the experiment.

REFERENCES

Abdoun, T., Dobry, R., O'Rourke, T. D. and Goh, S. H. 2003. Pile response to lateral spreads: Centrifuge modeling. Journal of Geotechnical and Geoenvironmental Engineering, ASCE, **129**(10): 869-878.

Anagnostopoulos, C. and Georgiadis, M. 1993. Interaction of axial and lateral pile responses. Journal of Geotechnical Engineering Division, ASCE, **119**(4): 793-798.

Aubeny, C. P., Han, S. W. and Murff, J. D. 2003. Inclined load capacity of suction caissons. International Journal for Numerical and Analytical Methods in Geomechanics, **27**(14): 1235-1254.

Bransby, M. F. and Springman, S. M. 1997. Centrifuge modelling of pile groups adjacent to surcharge loads. Soils and Foundations, **37**(2): 39-49.

Broms, B. 1964. Lateral resistance of piles in cohesionless soils. Journal of Soil Mechanics and Foundation Engineering Division, ASCE, **90**(3): 123-156.

Cai, F. and Ugai, K. 2003. Response of flexible piles under laterally linear movement of the sliding layer in landslides. Canadian Geotechnical Journal, **40**(1): 46-53.

Carrubba, P., Maugeri, M. and Motta, E. 1989. Esperienze in vera grandezza sul comportamento di pali per la stabilizzaaione di un pendio. *In* Proceedings of XVII Convegno Nazionale di Geotechica, Assn. Geotec, Italiana, **1**: 81-90.

Chen, L. T. and Poulos, H. G. 1997. Piles subjected to lateral soil movements. Journal of Geotechnical and Geoenvironmental Engineering, ASCE, **123**(9): 802-811.

Chmoulian, A. and Rendel, H. 2004. Briefing: Analysis of piled stabilization of landslides. Proceedings of the Institution of Civil Engineers, Geotechnical Engineering, **157**(2): 55-56.

Chow, Y. K. 1996. Analysis of piles used for slope stabilization. International Journal for Numerical and Analytical Methods in Geomechanics, **20**(9): 635-646.

Esu, F. and D'Elia, B. 1974. Interazione terreno-struttura in un palo sollecitato dauna frana tipo colata. Rivista Italiana di Geotechica, **8**(1): 27-38.

Frank, R. and Pouget, P. 2008. Experimental pile subjected to long duration thrusts owing to a moving slope. Geotechnique, **58**(8): 645-658.

Fukuoka, M. 1977. The effects of horizontal loads on piles due to landslides. *In* Proceedings 9th International Conference on Soil Mechanics and Foundation Engineering, Speciality session 10, Tokyo, **1**: 27-42.

Guo, W. D. 2003. A simplified approach for piles due to soil movement. *In* Proceedings of 12th Panamerican Conference on Soil Mechanics and Geotechnical Engineering, Cambridge, Massachusettes, USA, Verlag Gluckauf GMBH. Essen (Germany), **2**: 2215-2220.

Guo, W. D. 2008a. Laterally loaded rigid piles in cohesionless soil. Canadian Geotechnical Journal, **45**(5): 676-697.

Guo, W. D. 2008b. A pragmatic approach for rigid passive piles in sand. Journal of Geotechnical and Geoenvironmental Engineering, ASCE: resubmitted on October 13 2008.

Guo, W. D. 2009. Nonlinear response of slope stabilising piles. Canadian Geotechnical Journal: Under review, submitted on June 15, 2009.

Guo, W. D. and Ghee, E. H. 2004. Model tests on single piles in sand subjected to lateral soil movement. *In* Proceedings of the 18th Australasian Conference on the Mechanics of Structures and Materials, Perth, Australia, A. A. Balkema, Rotterdam, The Netherlands, **2**: 997-1003.

Guo, W. D. and Ghee, E. H. 2005. A preliminary investigation into the effect of axial load on piles subjected to lateral soil movement. *In* Proceedings of 1st International Symposium on Frontiers in Offshore Geotechnics, Perth, Australia, Tayler & Francis, **1**: 865-871.

Guo, W. D. and Lee, F. H. 2001. Load transfer approach for laterally loaded piles. International Journal for Numerical and Analytical Methods in Geomechanics, **25**(11): 1101-1129.

Guo, W. D. and Qin, H. Y. 2006. Vertically loaded piles in sand subjected to triangular profiles of soil movements. *In* Proceedings of 10th International Conference on Piling and Foundations, Amsterdam, Netherland **1**: paper no. 1371.

Guo, W. D., Qin, H. Y. and Ghee, E. H. 2006. Effect of soil movement profiles on vertically loaded single piles. *In* Proceedings of International Conference on Physical Modelling in Geotechnics, Hong Kong, China, Taylor & Francis Group plc, London, UK, **2**: 841-846.

Ito, T. and Matsui, T. 1975. Methods to estimate lateral force acting on stabilizing piles. Soils and Foundations, **15**(4): 43-59.

Kalteziotis, N., Zervogiannis, H., Frank, R., Seve, G. and Berche, J.-C. 1993. Experimental study of landslide stabilization by large diameter piles. *In* Proceedings of International Symposium on Geotechnical Engineering of Hard Soils-soft Rocks, Athens, A. A. Balkema, Rotterdam, The Netherlands, **2**: 1115-1124.

Karthigeyan, S., Ramakrishna, V. V. G. S. T. and Rajagopal, K. 2007. Numerical investigation of the effect of vertical load on the lateral response of piles. Journal of Geotechnical and Geoenvironmental Engineering, ASCE, **133**(5): 512-521.

Knappett, J. A. and Madabhushi, S. P. G. 2009. Influence of axial load on lateral pile response in liquefiable soils. Part II: numerical modelling. Geotechnique, **doi**(?): 10.1680/geot.8.010.3750.

Leung, C. F., Chow, Y. K. and Shen, R. F. 2000. Behaviour of pile subject to excavation-induced soil movement. Journal of Geotechnical and Geoenvironmental Engineering, American Society of Civil Engineers, **126**(11): 947-954.

Meyerhof, G. G., Mathur, S. K. and Valsangkar, A. J. 1981. Lateral resistance and deflection of rigid wall and piles in layered soils. Canadian Geotechnical Journal, **18**(?): 159-170.

Meyerhof, G. G., Yalcin, A. S. and Mathur, S. K. 1983. Ultimate pile capacity for eccentric inclined load. Journal of Geotechnical Engineering Division, ASCE, **109**(3): 408-423.

Pan, J. L., Goh, A. T. C., Wong, K. S. and Teh, C. I. 2002. Ultimate soil pressure for piles subjected to lateral soil movements. Journal of Geotechnical and Geoenvironmental Engineering, ASCE, **128**(6): 530-535.

Poulos, H. G. 1995. Design of reinforcing piles to increase slope stability. Canadian Geotechnical Journal, **32**(5): 808-818.

Poulos, H. G., Chen, L. T. and Hull, T. S. 1995. Model tests on single piles subjected to lateral soil movement. Soils and Foundations, **35**(4): 85-92.

Scott, R. F. 1981. Foundation analysis. N. J., Prentice Hall, Englewood Cliffs.

Smethurst, J. A. and Powrie, W. 2007. Monitoring and analysis of the bending behaviour of discrete piles used to stabilise a railway embankment. Geotechnique, **57**(8): 663-677.

Stewart, D. P., Jewell, R. J. and Randolph, M. F. 1994. Design of piled bridge abutment on soft clay for loading from lateral soil movements. Geotechnique, **44**(2): 277-296.

Viggiani, C. 1981. Ultimate lateral load on piles used to stabilise landslide. *In* Proceedings of 10th International Conference on Soil Mechanics and Foundation Engineering, Stockholm, Sweden, **3**: 555-560.

Figure Captions

Table 1. Summary of 14 typical pile tests

Test description	Frame movement at ground surface w_f (mm)	Maximum bending moment M_{max} (kNmm)		Depth of M_{max}, d_{max} (mm)	Max shear force, T_{max} (N)		Pile deflection at groundline, y_t (mm)	L_m/L_s (mm)	Remarks
		Tension side	compression side		Stable layer	Sliding layer			
TS32-0 (s_b = 340)*	60/80	63.8/81.0		400	266.9/327.7	266.6/325.8	11.5/14.8	200/500	Pile location
TS32-0 (s_b = 660)*	60/80	30.0/40.0		400	114.9/150.3	120.4/153.7	7.8/10.8	200/500	
TS32-0 (L_m =200)	60/70	39.3/49.7	-34.2/-45.0	370	147.2/183.8	159.8/201.1	7.1/10.3	200/500	Standard Tests (s_b = 500)
TS32-294	60/90	29.8/78.6	-26.8/-76.5	375	108.5/295.5	98.0/279.9	5.4/13.1	200/500	
TS50-0	60/80	45.8/89.2	-37.9/-80.2	380	191.9/363.9	180.3/355.7	2.9/7.2	200/500	
TS50-294	60/80	58.5/115.6	-59.2/-120.0	400	229.6/445.5	241.4/467.5	3.5/7.3	200/500	
TD32-0	120	119.5	-112.1	450	495.9	414.8	58.7	350/350	
TD32-294	120	124.6	-117.5	465	532.4	463.5	73.8	350/350	
TD50-0	120	93.2	-84.4	450	393.8	353.1	58.9	350/350	
TD50-294	120	143.0	-135.1	450	577.6	453.4	67.5	350/350	
T32-0 (L_m = 125)	40/60	5.2/5.7		325	18.9/18.2	22.8/22.5	0.5/0.6	125/575	Varying sliding depth (s_b = 500)
T32-0 (L_m =250)	80/120	62.6/123.5		450	258.1/509.4	233.9/457.3	22.4/47.7	250/450	
T32-0 (L_m =300)	100/150	115.3/175.0		450	450.6/675.2	399.4/619.6	25.1/54.8	300/400	
T32-0 (L_m =350)	120/150	118.1/140.0		475	471.7/557.3	406.7/535.3	42.2/73.9	350/350	

Table 2. Frame movement (w_f) versus depth of moving soil (L_m)

Profile	Frame movement, w_f (mm)	10	20	30	50	70	110	120
Triangular (Final L_m = 200 mm)	Number of fully Mobilized frames	2	3	4	6	8	8	8
	Depth of soil movement, L_m (mm)	50	75	100	150	200	200	200
	Sliding depth ratio, R_L	0.07	0.10	0.14	0.21	0.29	0.29	0.29
Triangular (Final L_m = 350 mm)	Frame movement, w_f (mm)	60	70	80	90	100	110	120
	Number of fully Mobilized frames	8	9	10	11	12	13	14
	Depth of soil movement, L_m (mm)	200	225	250	275	300	325	350
	Sliding depth ratio, R_L	0.29	0.32	0.36	0.39	0.43	0.46	0.50

Table 3. Calculation for 'translating' pile test TD32-0 and T32-0(L_m = 350 mm,)

Input data			Calculated [a]		Measured M_{max}(kNmm)	
w_f (mm)	G_s (kPa)	R_L	T_{max} (kN)	M_{max} (kNm)	T32-0	TD32-0
30	14	0.1270	0	0	0.86	3.66
40	14	0.1693	0.018	4.62	2.78	8.80
50	14	0.2116	0.080	20.04	11.68	26.37
60	14	0.2540	0.142	35.45	21.69	44.42
70	14	0.2963	0.203	50.86	38.47	56.56
80	14	0.3386	0.265	66.27	63.96	57.50
90	14	0.3809	0.327	81.68	84.23	68.40
100	14	0.4233	0.388	97.09	97.51	85.17
110	14	0.4656	0.450	112.50	106.98	96.56
120	14	0.6398	0.512	127.92	118.12	119.50
150 [b]	*14*	*0.7997*	*0.697*	*174.15*	*139.78*	
Note	[a] w_i = 37 mm, γ = 0.048, k/G_s = 2.516, L = 0.7 m, d = 32mm [b] Trapezoid movement profile					

Table 4. Calculation for 'rotating' tests (Poulos et al. 1995)

Input data				Calculated				Measured
Embedded length L (mm)	w_f (mm)	G_s (kPa)	R_L	Factor γ (= 1.05d/L)	k/G_s	T_{max} (kN)	M_{max} (kNmm)	M_{max} (kNmm)
525	37	5.25	0.38	0.05000	2.54	0.0648	*13.62*	8.0
575	37	5.75	0.43	0.04565	2.48	0.0760	*17.47*	17.4
625	37	6.25	0.48	0.04200	2.43	0.0879	*21.97*	25.0
675	60	6.75	0.52	0.03889	2.39	0.1631	44.03	44.2
625	60	6.25	0.56	0.04200	2.43	0.1425	35.63	36.1
575	60	5.75	0.61	0.04565	2.48	0.1232	28.33	25.5
525	60	5.25	0.67	0.05000	2.54	0.1051	22.08	15.8
475	60	4.75	0.74	0.05526	2.61	0.0884	16.79	7.1
425	60	4.25	0.82	0.06176	2.69	0.0729	12.39	3.0
375	60	3.75	0.93	0.07000	2.79	0.0588	8.82	0.8

Table 5 $M_{max}/(T_{max}L)$ determined for field tests

Piles			Soil		Measured			References
D/t [a] (mm)	E_p [a] (GPa)	L_1/L_2 [a] (m)	k_1/k_2 [a] (MPa)	L_{c1}/L_{c2} [a] (m)	M_{max} [a, b] (kNm)	T_{max} [a] (kN)	$\frac{M_{max}}{T_{max}L}$ [b]	
790/395	20	7.5/22.5	$\frac{8.0}{8.0}$	19.5/19.5	903	310	0.388	Esu and D'Elia (1974)
1200/600	20	9.5/13.0	$\frac{15}{15}$	12.7/12.7	2,250	600	0.395	Carrubba et al (1989)
630/315	28.45	2.5/10.0	$\frac{14.4}{28.8}$	23.1/23.1	60.2	56-60 [c]	0.40-0.43	Leung et al (2000) (2.5 m)
630/315	28.45	3.5/9.0	$\frac{14.4}{28.8}$	23.1/23.1	73.8	65-85 [c]	0.25-0.32	Leung et al (2000) (3.5 m)
630/315	28.45	4.5/8.0	$\frac{14.4}{28.8}$	23.1/23.1	81.2	72-100 [c]	0.18-0.25	Leung et al (2000) (4.5 m)
318.5/6.9	210	11.2/12.8	$\frac{5.0}{8.0}$	6.3/5.6	165.2	144-150 [c]	0.18-0.20	Hataori-2 [d]
318.5/6.9	210	8.0/9.0	$\frac{5.0}{15.0}$	6.3/4.9	65.7	70-71.2 [c]	0.15-0.19	Hataori-3 [d]
318.5/6.9	210	6.5/7.5	$\frac{5.0}{8.0}$	6.3/5.6	197.2	143-300 [c]	0.10-0.25	Kamimoku-4 [d]
318.5/6.9	210	4.0/6.0	$\frac{5.0}{8.0}$	6.3/5.6	290.3	231-250 [c]	0.18-0.22	Kamimoku-6 [d]
300/60	20	7.3/5.7	$\frac{6.0}{10.0}$	3.2/2.8	69.5	40-56.2 [c]	0.38-0.62	Katamachi-B [d]
915/19	31.1 [e]	6.8/4.2	$\frac{8.8}{8.8}$	9.7/9.7	$\frac{901.9}{312.5}$ [f]	$\frac{532.6}{221.9}$ [f]	$\frac{0.249}{0.207}$ [f]	$\frac{5Nov,86}{4Nov,86}$ [g]
					$\frac{1102.3}{536.6}$ [f]	$\frac{642.3}{369.5}$ [f]	$\frac{0.252}{0.214}$ [f]	$\frac{11Nov,88}{10Nov,88}$ [g]
					$\frac{1473.5}{544.3}$ [f]	$\frac{796.4}{378.5}$ [f]	$\frac{0.272}{0.211}$ [f]	$\frac{1Oct,92}{30Sept,92}$ [g]
					$\frac{1434.2}{756.1}$ [f]	$\frac{834.7}{487.0}$ [f]	$\frac{0.253}{0.228}$ [f]	$\frac{6July,95}{5July,95}$ [g]

[a] Guo (2009); D = outside diameter; t = wall thickness; E_p = Young's modulus of pile; L_1/L_2 = thickness of sliding/stable layer; k_1/k_2 = subgrade modulus of sliding/stable layer. L_{c1}/L_{c2} = equivalent length for rigid pile in sliding/stable layer. In the estimation, G_{si} was simply taken as $k_i/3$. [b] M_{max} = measured maximum bending moment; L = the smallest value of L_i and L_{ci}. [c] estimated using elastic and elastic-plastic solutions against measured bending moment and pile deflection and soil movement profiles; [d] Cai and Ugai (2003); [e] E_pI_p (flexural stiffness) = 1,070 MN-m^2; [f] all for sliding layer; [g] Frank and Pouget (2008).

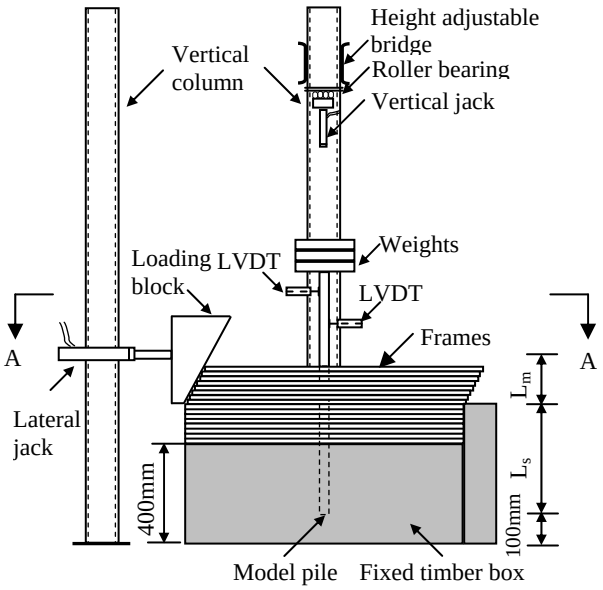

(a) Elevation view

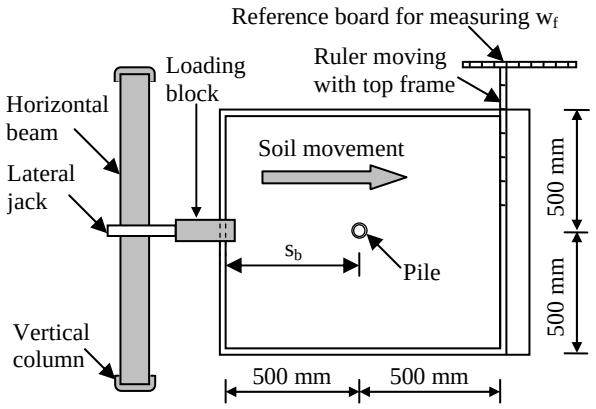

(b) Initial plan view (A-A)

Fig. 1. Schematic diagram of shear box

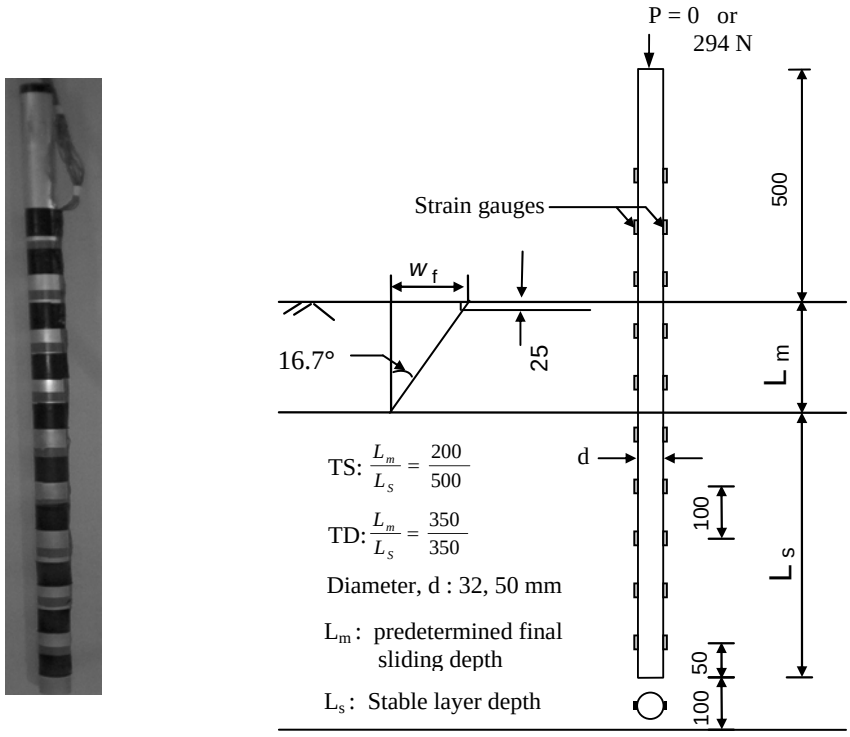

(a) An instrumented model pile (b) Schematic diagram of testing

Fig. 2. Schematic test of a pile subjected to triangular loading block

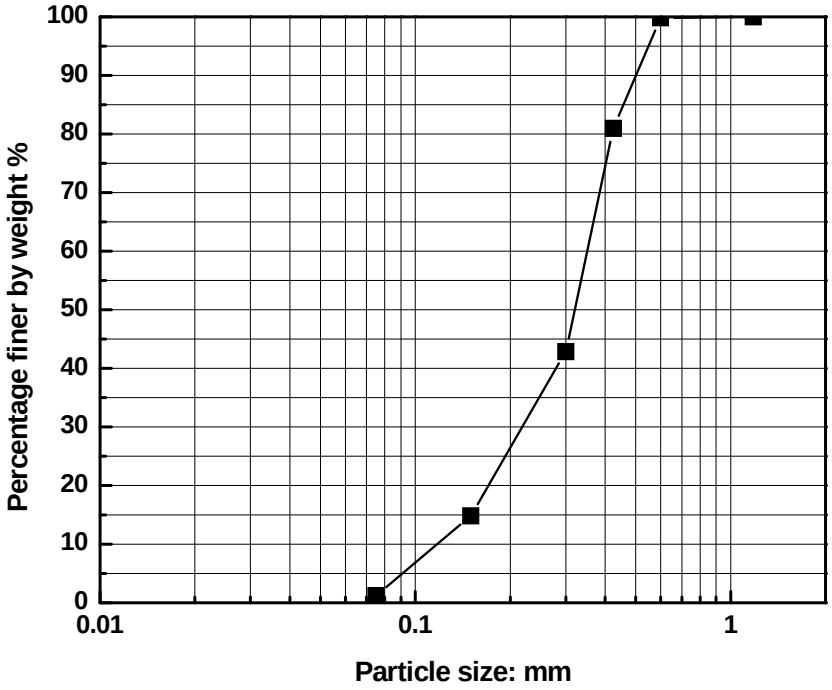

Fig. 3. Particle size distribution of used sand

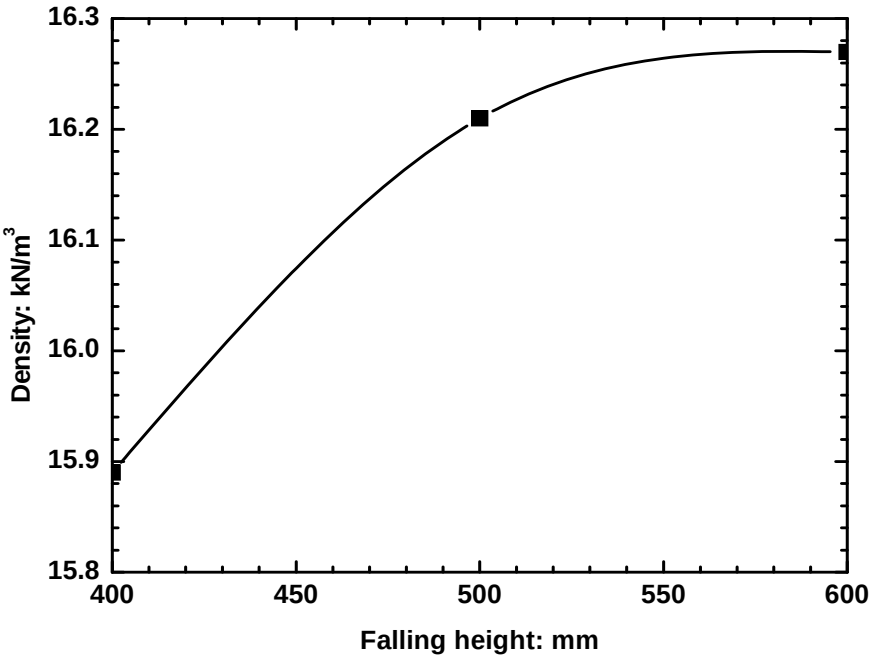

Fig. 4 Relationship between falling height and sand density

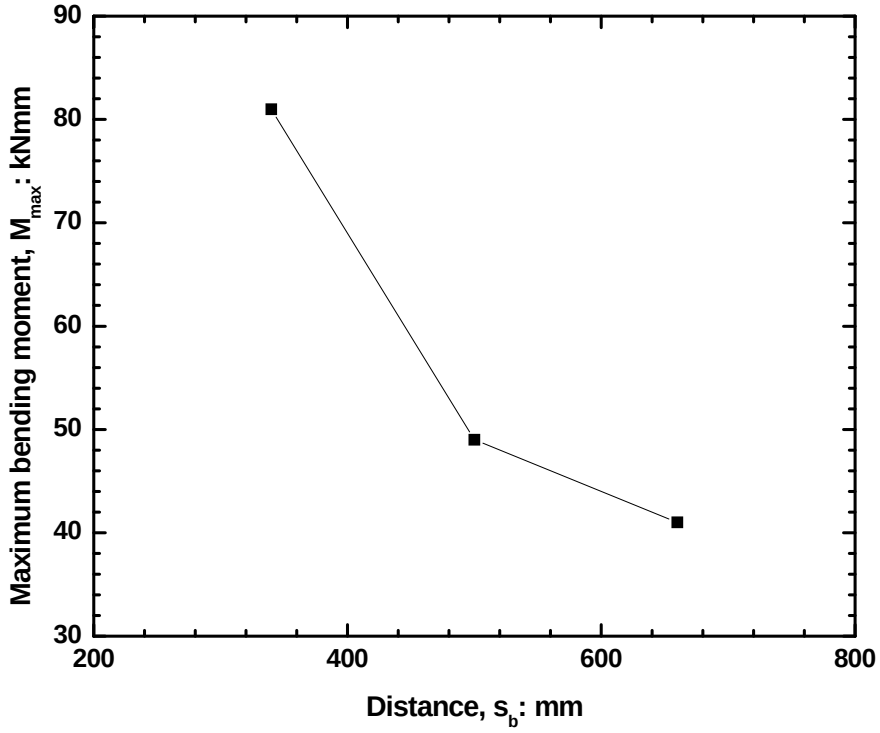

Fig. 5. Variation of M_{max} versus distance of pile from loading side, s_b

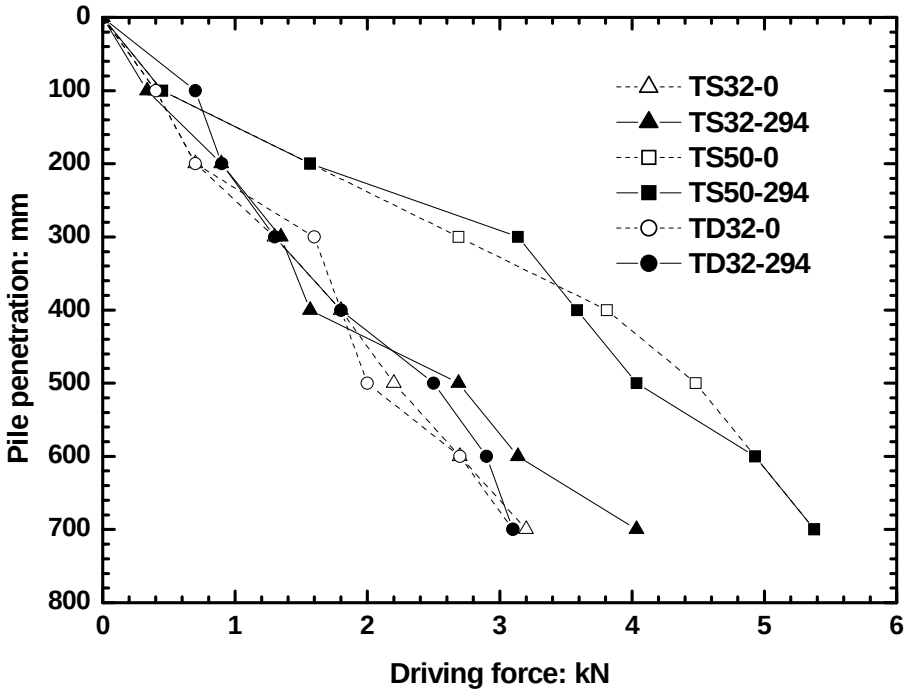

Fig. 6. Jack-in resistance measured during pile installation

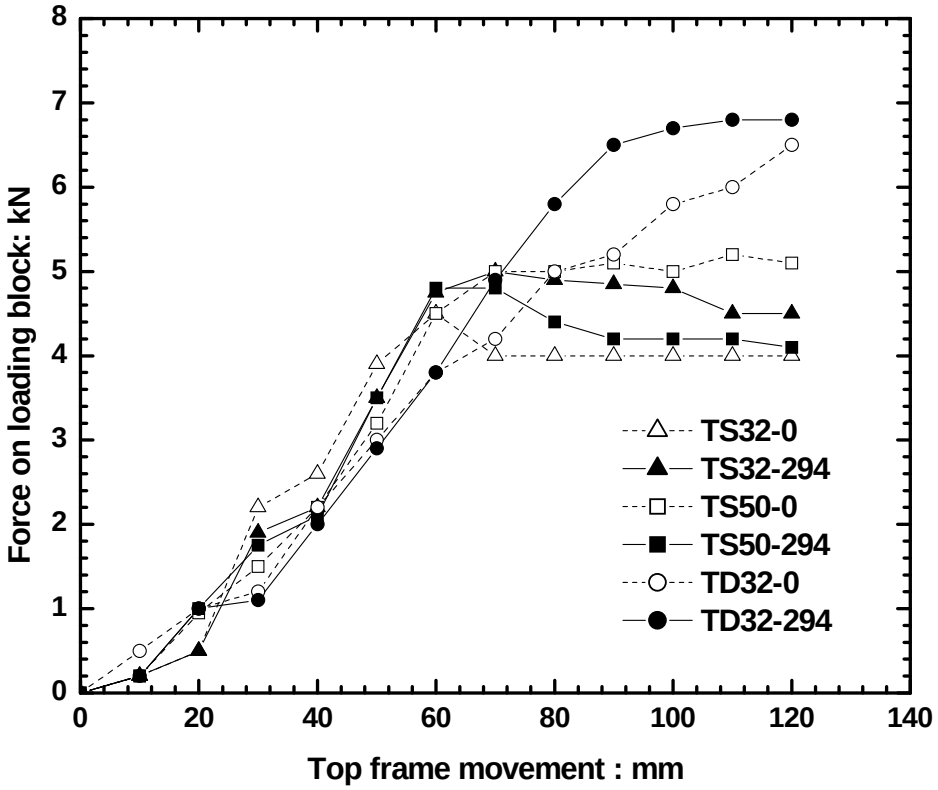

Fig. 7. Total applied force on frames against frame movements

w_f: mm (a) 10 (b) 20 (c) 30 (d) 50 (e) 70 (f) 110 (g) 140

(h) Overview of sand heaves at w_f = 150 mm

Fig. 8. Progressively moving sand induced by a triangular loading block

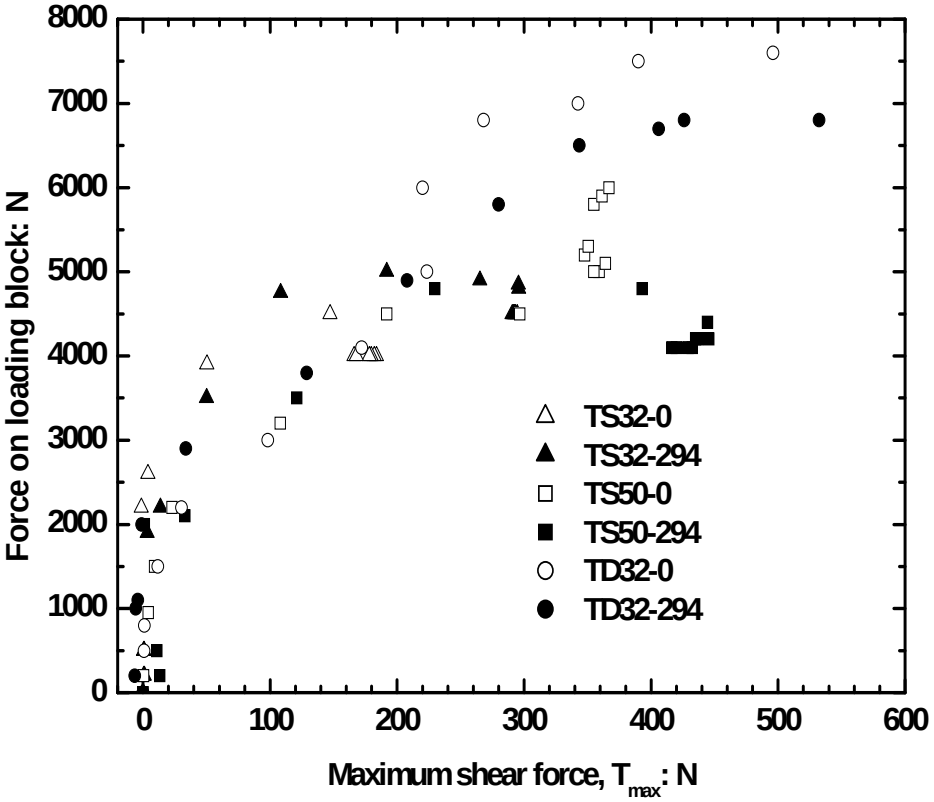

Fig. 9. Variation of maximum shear force versus lateral force on loading block

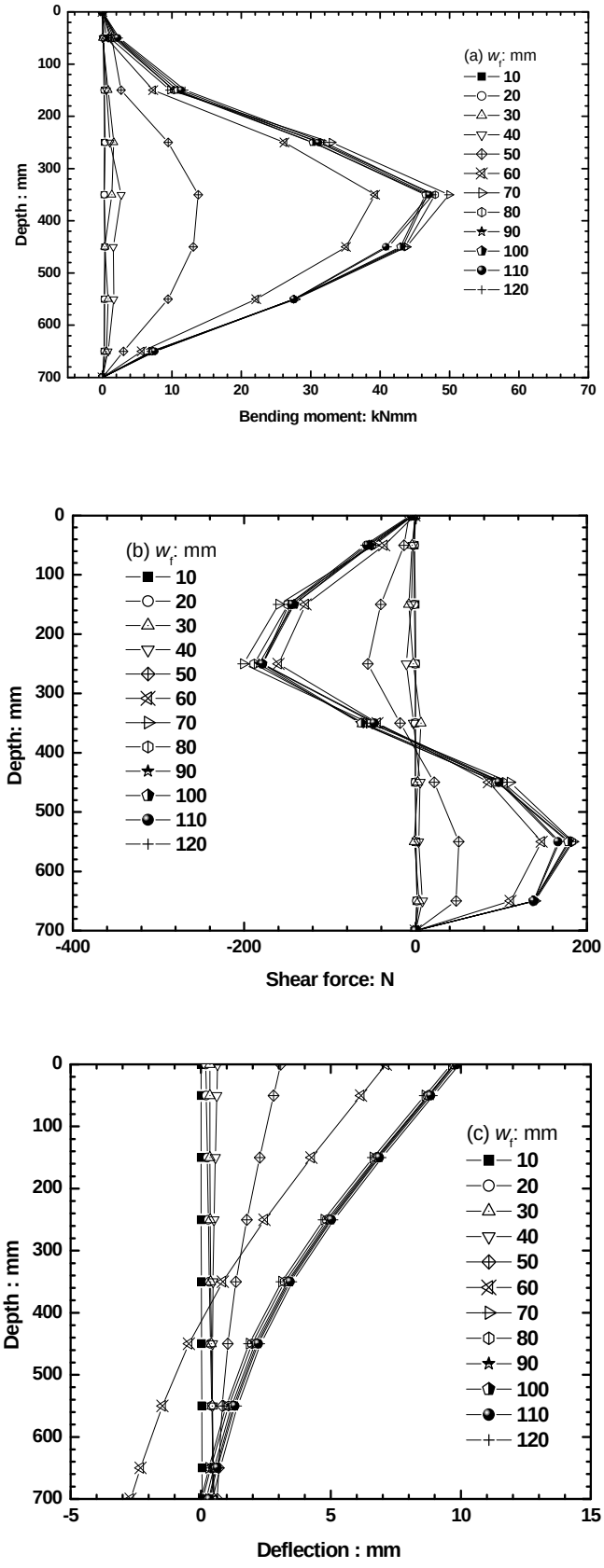

Fig. 10. Response of pile during TS32-0

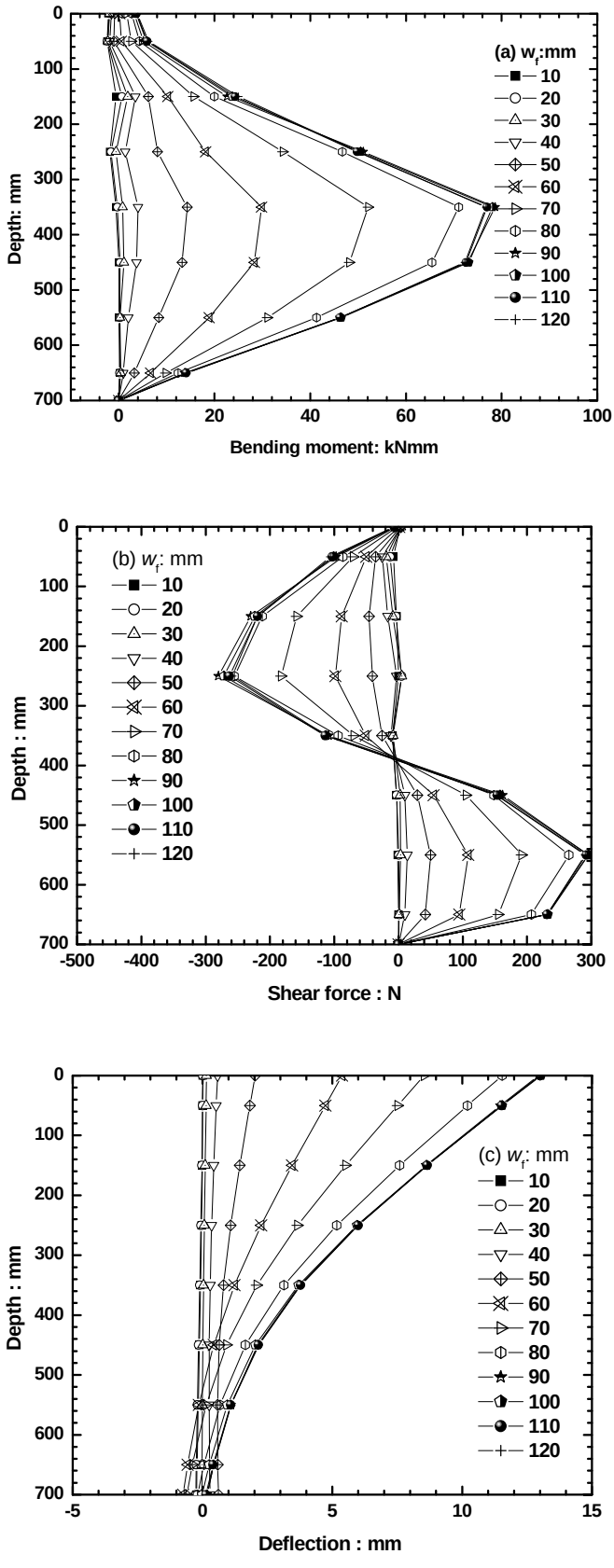

Fig. 11. Response of pile during TS32-294

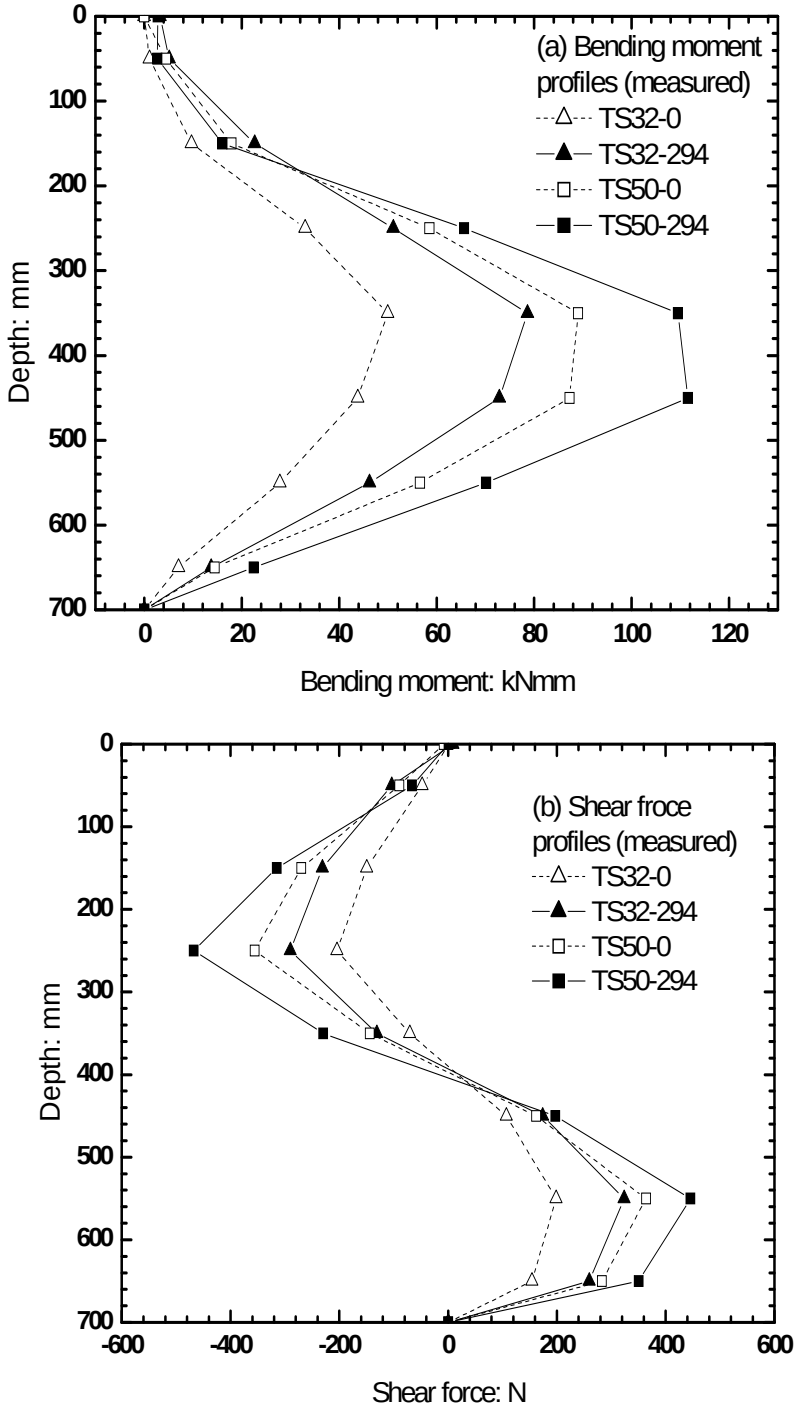

Fig. 12. Maximum response profiles of piles (final sliding depth = 200 mm)

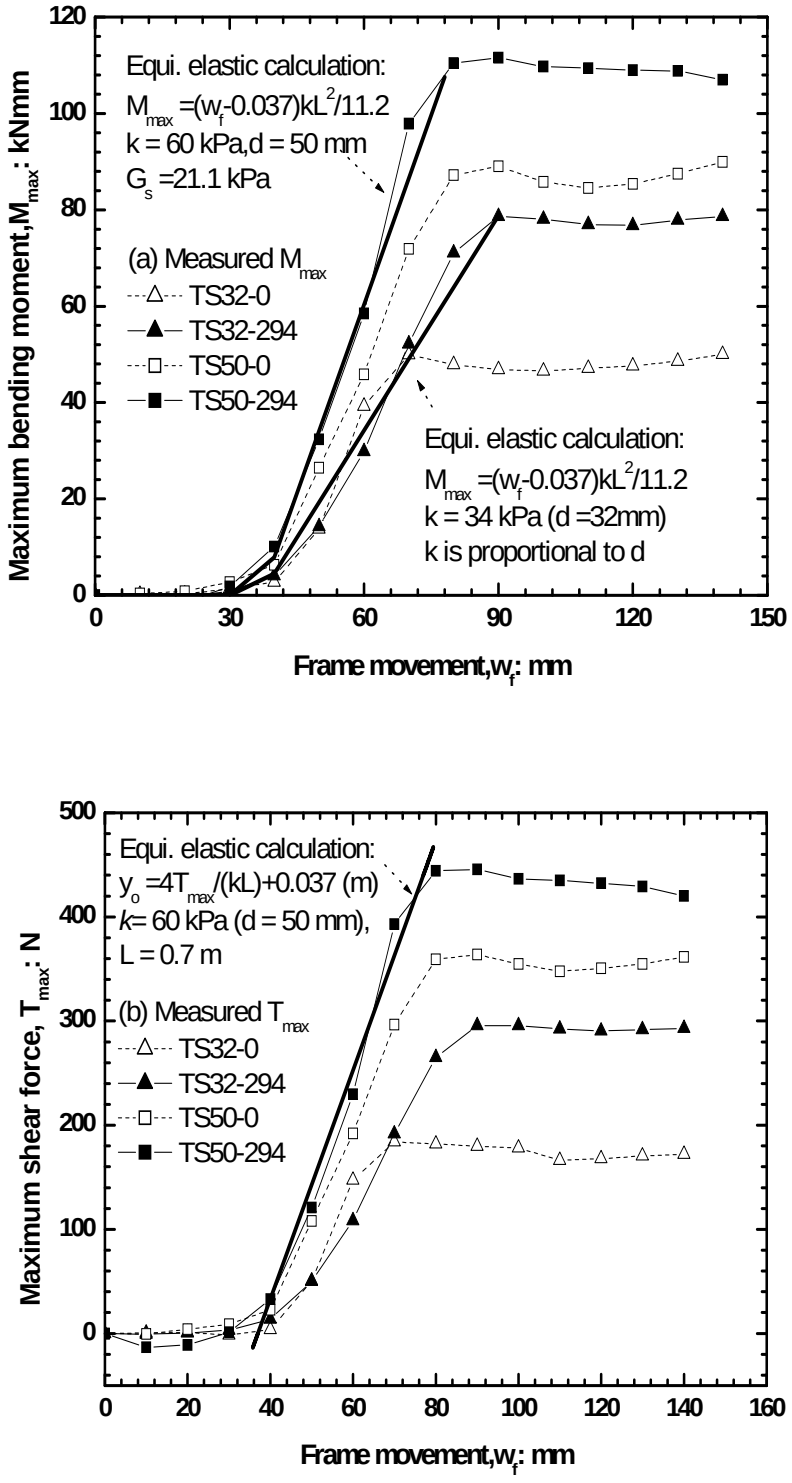

Fig. 13. Evolution of maximum response of piles (final sliding depth = 200 mm)

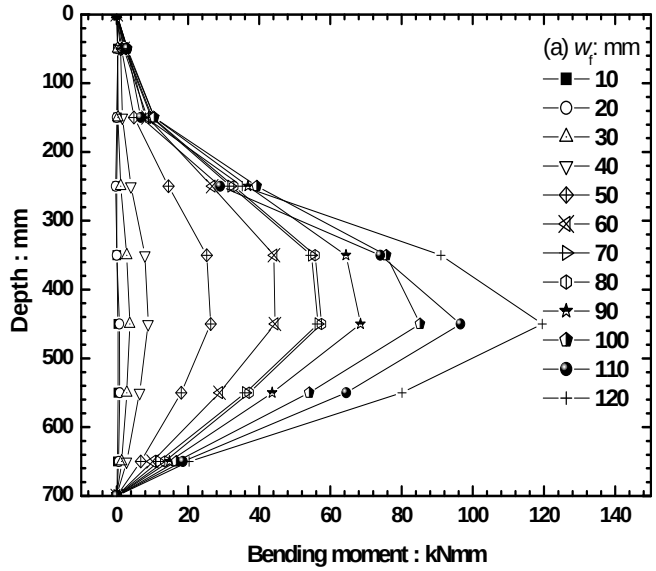

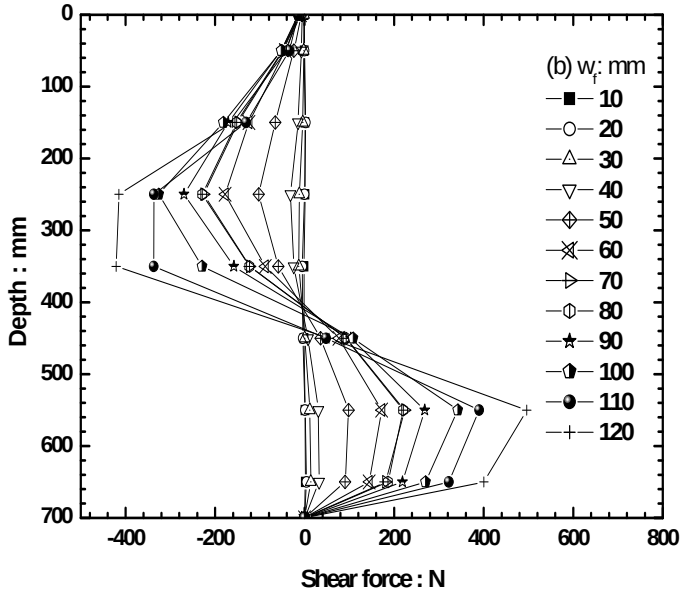

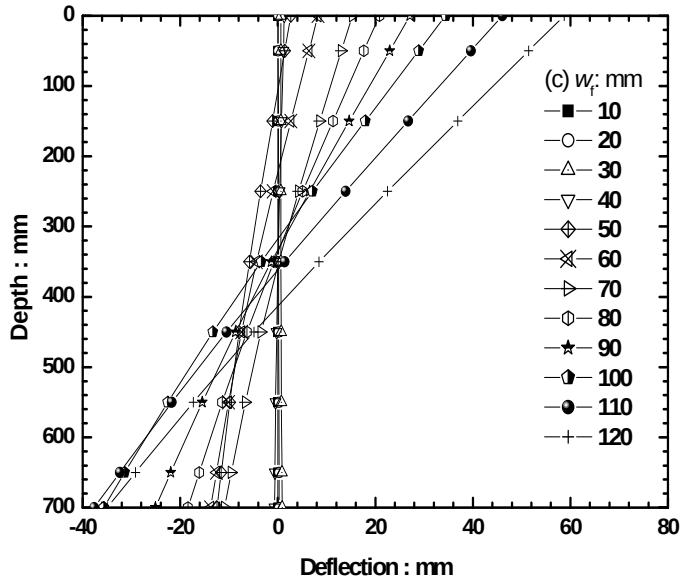

Fig. 14. Response of pile during TD32-0

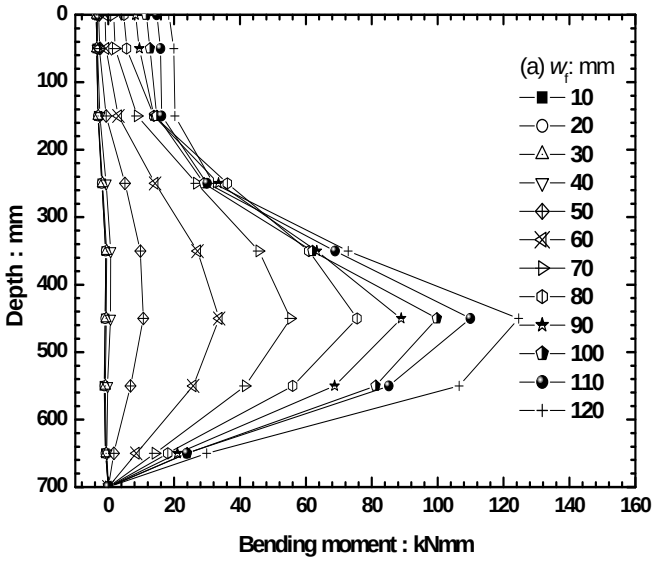

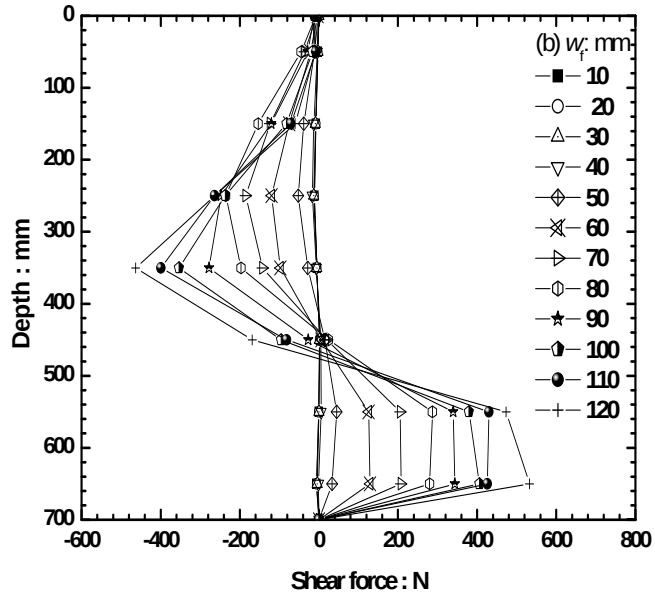

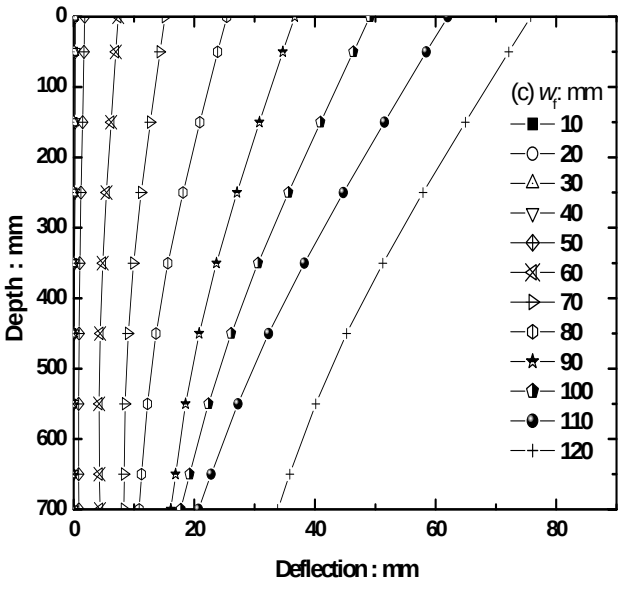

Fig. 15. Response of pile during TD32-294

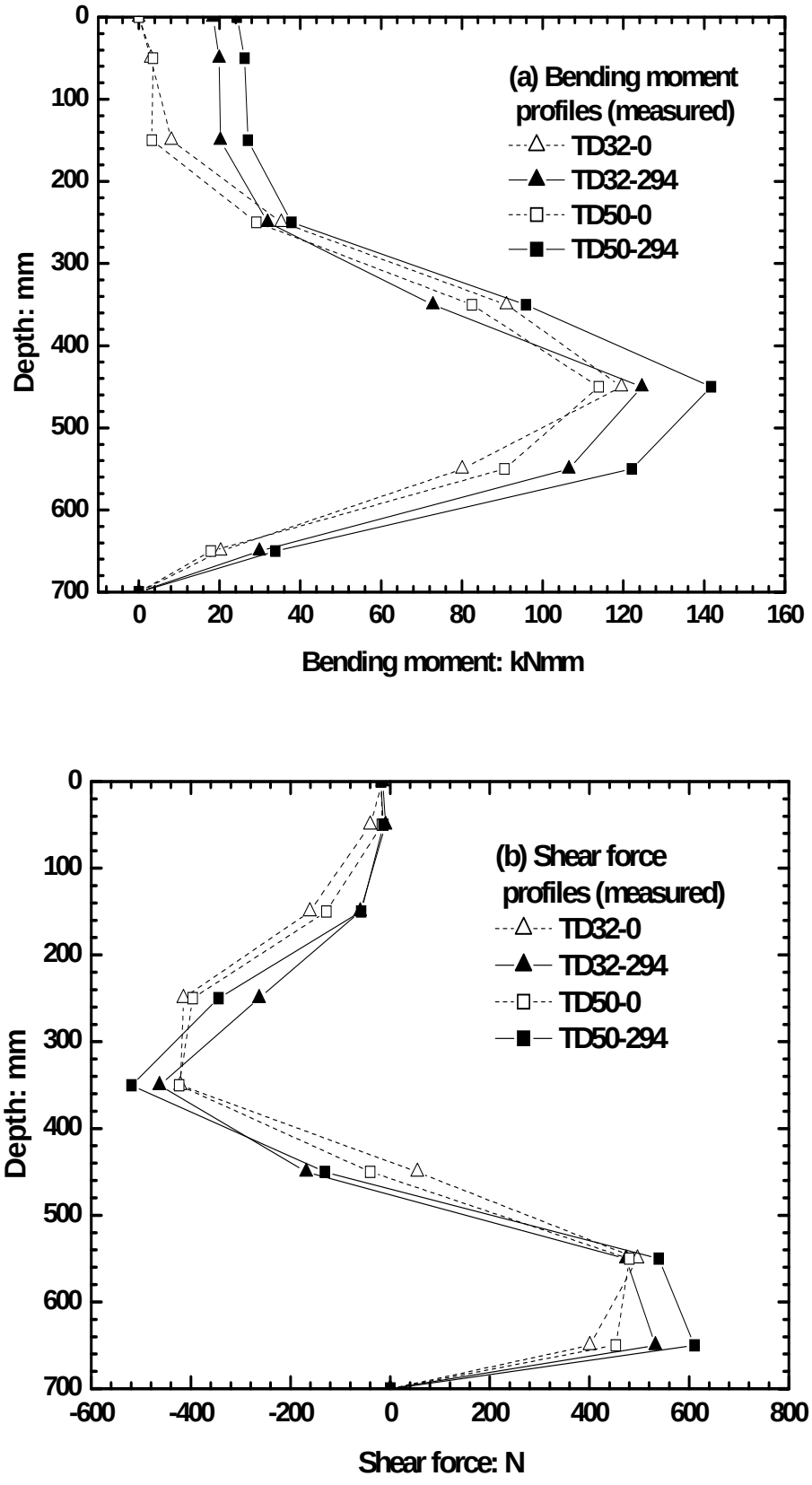

Fig. 16. Maximum response profiles of piles (final sliding depth = 350 mm)

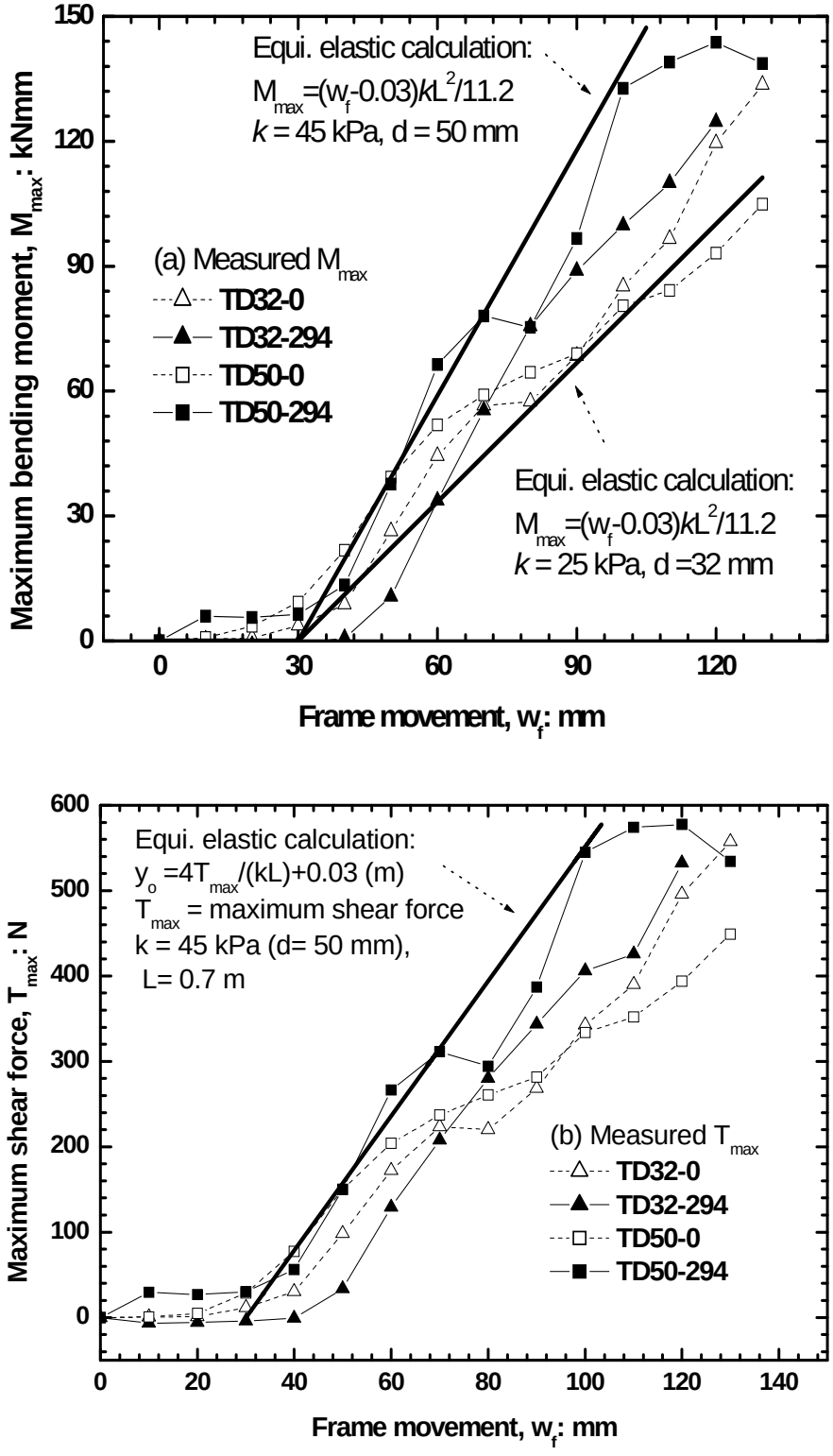

Fig. 17. Evolution of maximum response of piles (final sliding depth = 350 mm)

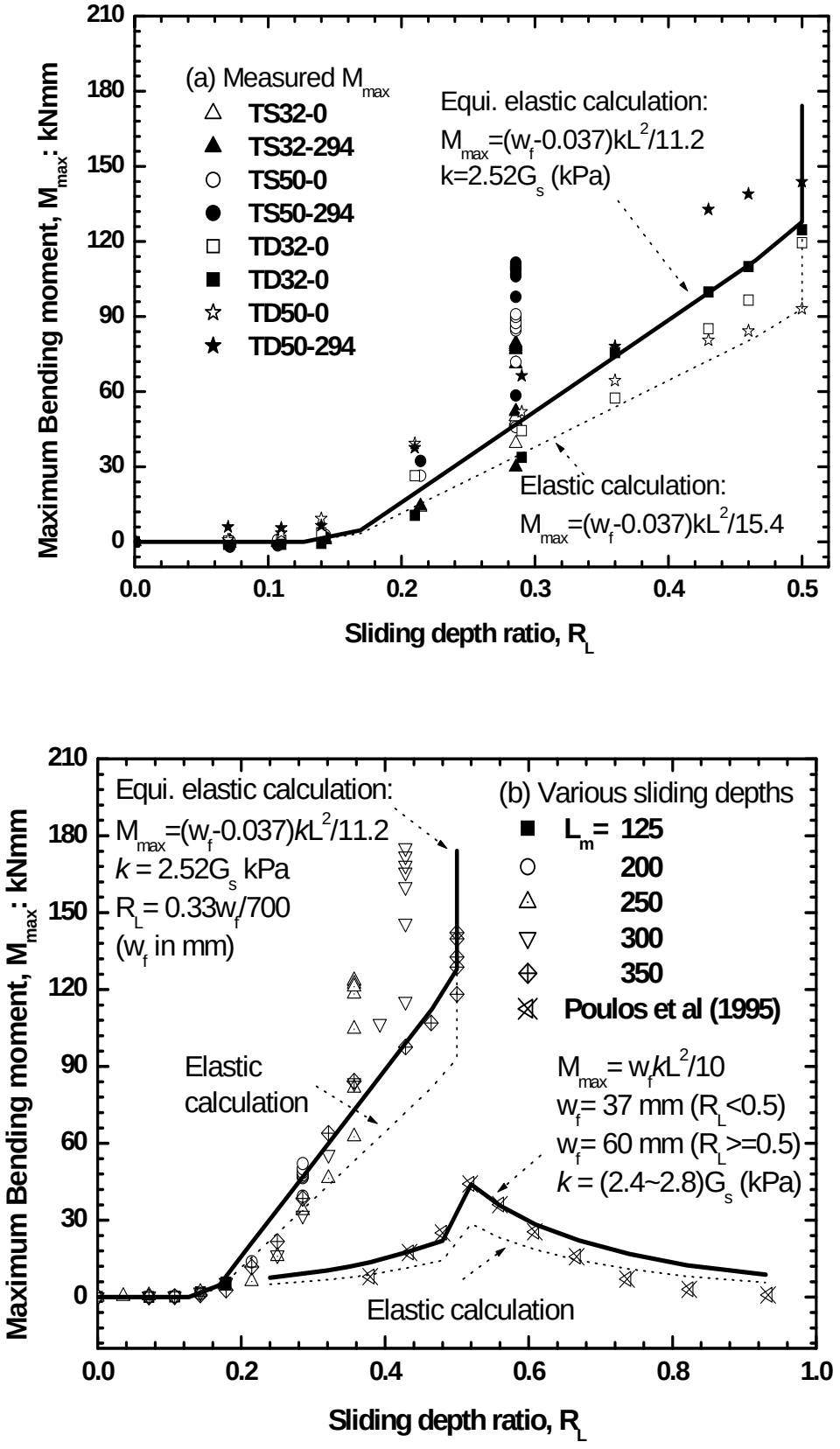

Fig. 18. Variation of maximum bending moment versus sliding depth ratio

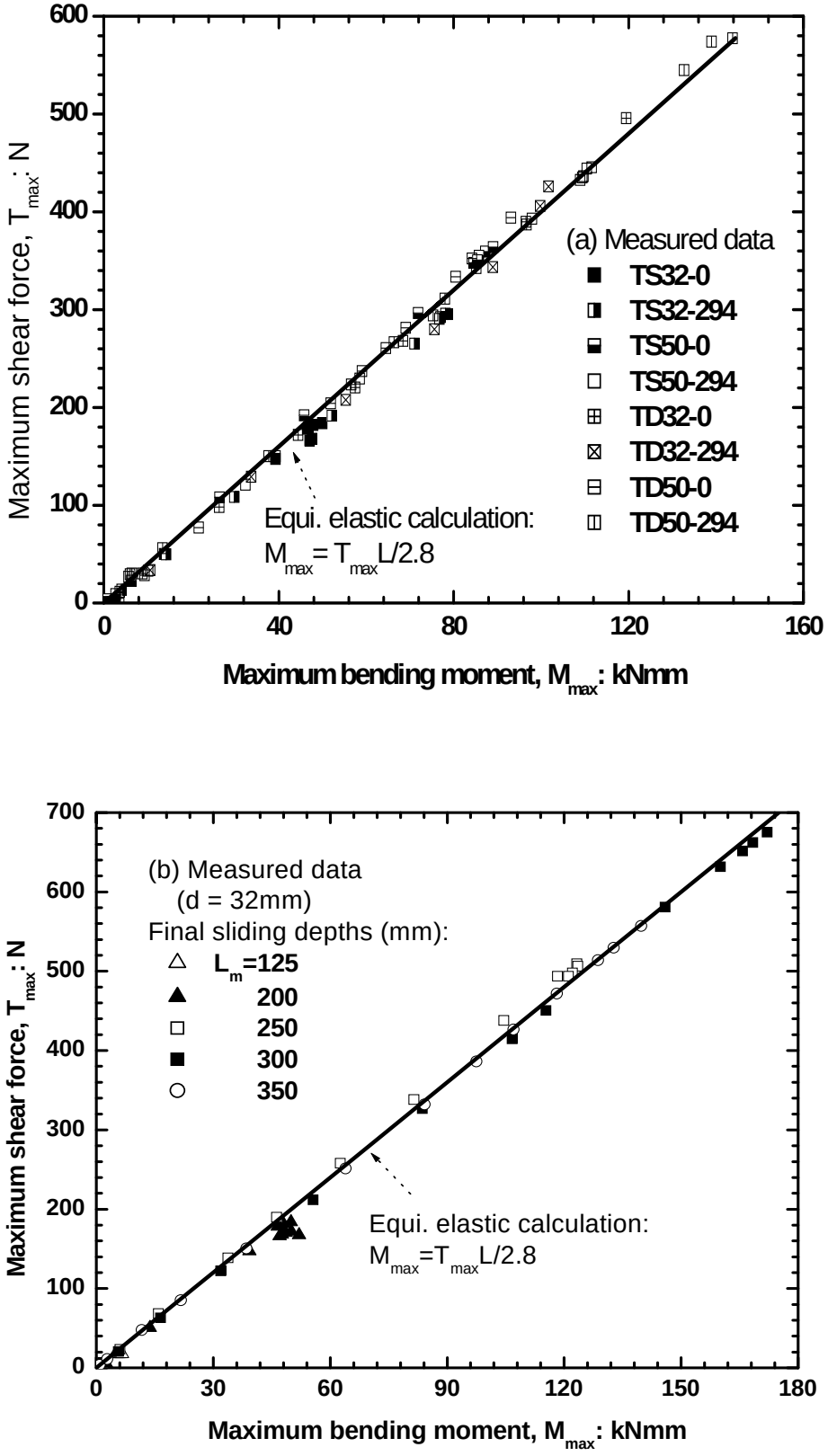

Fig. 19. Maximum shear force versus maximum bending moment

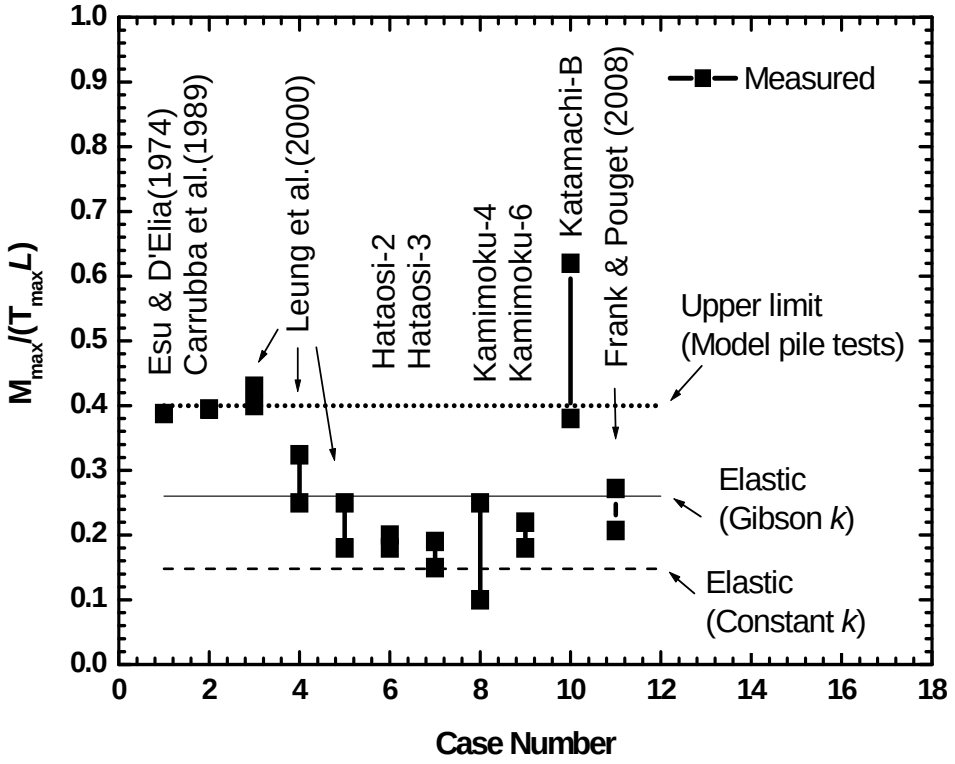

Fig. 20. Calculated versus measured ratios of $M_{max}/(T_{max}L)$

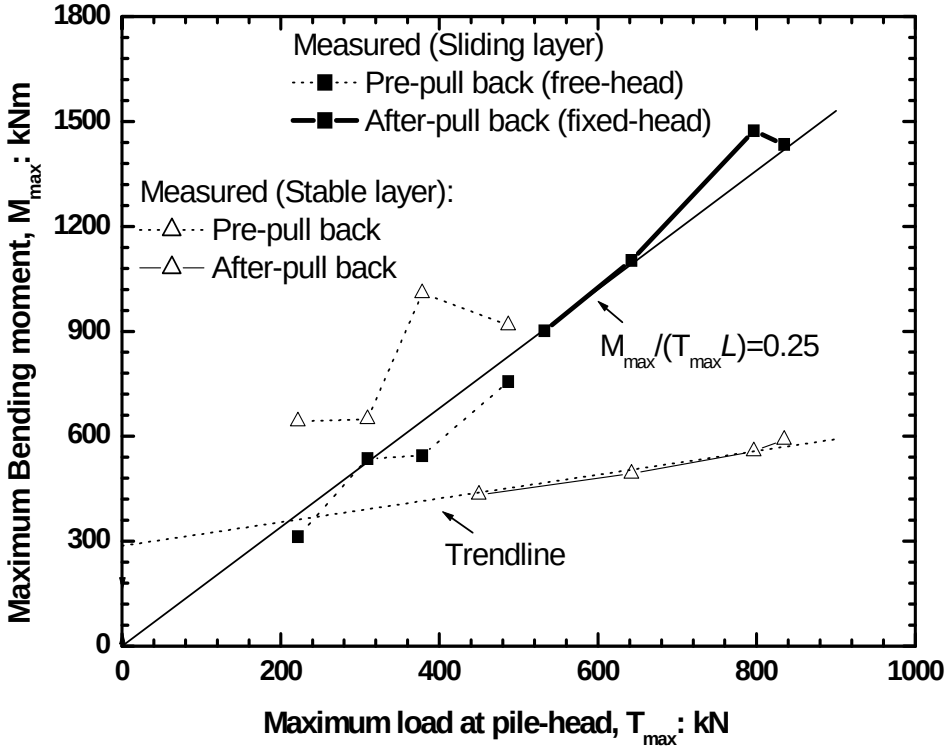

Fig. 21. Measured M_{max} and T_{max} (Frank and Pouget 2008)